Molecular Therapy
Methods & Clinical Development
Original Article

Evaluation of AAV vectors with tissue-specific or ubiquitous promoters in a mouse model of mucopolysaccharidosis type IVA

Shaukat A. Khan,[1] Jose Victor Álvarez,[1,2] F.N.U. Nidhi,[1,3] Eliana Benincore-Florez,[1] and Shunji Tomatsu[1,4,5,6]

[1]Department of Biomedical Research, Nemours Children's Health, Wilmington, DE 19803, USA; [2]Department of Pediatrics, Hospital Clínico Universitario de Santiago de Compostela, Health Research Institute of Santiago de Compostela (IDIS), CIBERER, MetabERN, 15706 Santiago de Compostela, Spain; [3]Department of Biological Sciences, University of Delaware, Newark, DE 19716, USA; [4]Department of Pediatrics, Shimane University, Izumo 693-8501, Japan; [5]Department of Pediatrics, Graduate School of Medicine, Gifu University, Gifu 501-1193, Japan; [6]Department of Pediatrics, Thomas Jefferson University, Philadelphia, PA 19107, USA

Mucopolysaccharidosis type IVA (MPS IVA) is caused by a deficiency of *N*-acetyl-galactosamine-6-sulfate sulfatase (GALNS), leading to the accumulation of keratan sulfate and chondroitin-6-sulfate and development of severe skeletal dysplasia. Enzyme replacement therapy and hematopoietic stem cell transplantation are current treatment options but have limited impact on bone lesions. In this study, we investigated adeno-associated virus (AAV)8 or AAV9 vectors with liver-specific thyroxine-binding globulin or liver-specific promoter-a modification of hAAT (LSPX), liver-muscle tandem (LMTP), liver-bone tandem (LBTP), and ubiquitous cytomegalovirus early enhancer/chicken β-actin (CAG) promoters in MPS IVA mice to compare therapeutic efficacy on biochemical markers and bone pathology. All vectors provided near- or supraphysiological levels of GALNS enzyme activity in plasma. Enzyme activities were also detected in various tissues, including bone. AAV9co-CAG, AAV9co-LMTP, and AAV9co-LBTP showed higher enzyme activities in the liver; however, AAV8co-CAG and AAV9co-LMTP have higher activities in most other tissues. All vectors normalized keratan sulfate levels in plasma, liver, and bone. Pathological analyses showed the reduction or complete absence of vacuolated cells in heart muscle and valves in all treated mice, while the AAV9co-LMTP vector most improved bone pathology. Overall, all studied vectors indicated a substantial improvement in biochemical parameters and pathology, and the AAV9co-LMTP vector demonstrated the best combined therapeutic efficacy.

INTRODUCTION

Mucopolysaccharidosis type IVA (MPS IVA, also known as Morquio A syndrome) is an autosomal recessive lysosomal disorder caused by a deficiency of a lysosomal enzyme, *N*-acetyl-galactosamine-6-sulfate sulfatase (GALNS).[1–4] Deficiency of the GALNS enzyme leads to the accumulation of glycosaminoglycans (GAGs), including chondroitin-6-sulfate (C6S) and keratan sulfate (KS), in systemic organs, especially bone and cartilage, resulting in pernicious skeletal dysplasia.[5–8] The clinical symptoms include pectus carinatum, kyphoscoliosis, genu valgum, laxity of joint, abnormal gait, and spinal cord compression. Patients require wheelchairs in their second decades of life due to severe muscle atrophy. Imbalance of growth leads to tracheal obstruction, resulting in high mortality and morbidity rates.[9–13] If the condition is left untreated, two-thirds of patients die of respiratory failures, while one-third of patients die of cardiac problems.[9] Enzyme replacement therapy (ERT) and hematopoietic stem cell transplantation (HSCT) are available treatments but have limited impact on bone and cartilage and on the removal of GAG from blood and tissue.[14–18]

Adeno-associated virus-(AAV)-mediated gene therapy has emerged as a novel treatment option for many genetic disorders and is being applied in many clinical trials. Gene transfer using AAV is effective in various animal models. AAV-mediated gene therapies in MPS I, II, IIIA, IIIB, and VI are under clinical trial (clinicaltrial.gov). We have previously reported that in models of MPS IVA, intravenous administration of an AAV8 vector encoding a human *GALNS* (*hGALNS*) under the control of a liver-specific promoter (thyroxine-binding globulin [TBG]) resulted in supraphysiological levels of the enzyme in plasma and partially ameliorated bone and cardiovascular pathologies.[19] Here, we have introduced further modifications to the AAV vector to enhance enzyme delivery to the bones and cartilage. Colella et al. demonstrated high and persistent transgene expression in non-dividing extra-hepatic tissues and prevention of anti-transgene immunity using AAV gene transfer by using tandem liver-muscle promoter in neonatal Pompe mice.[20] We have asked whether expressing the enzyme from the skeletal muscle could afford a better distribution to the cartilage and bones in MPS IVA. We present a comparison of liver-specific promoters, including the human alpha1-antitrypsin promoter (hAAT; LSPX), a ubiquitous cytomegalovirus early enhancer/chicken β-actin promoter (CAG); liver-muscle tandem promoter (LMTP), an ApoE enhancer/creatine kinase muscle promoter/hAAT liver promoter); and liver-bone tandem

Received 1 August 2024; accepted 11 March 2025;
https://doi.org/10.1016/j.omtm.2025.101447.

Correspondence: Shunji Tomatsu, MD, PhD, Department of Biomedical Research, Nemours Children's Health, Wilmington, DE 19803, USA.
E-mail: stomatsu@nemours.org

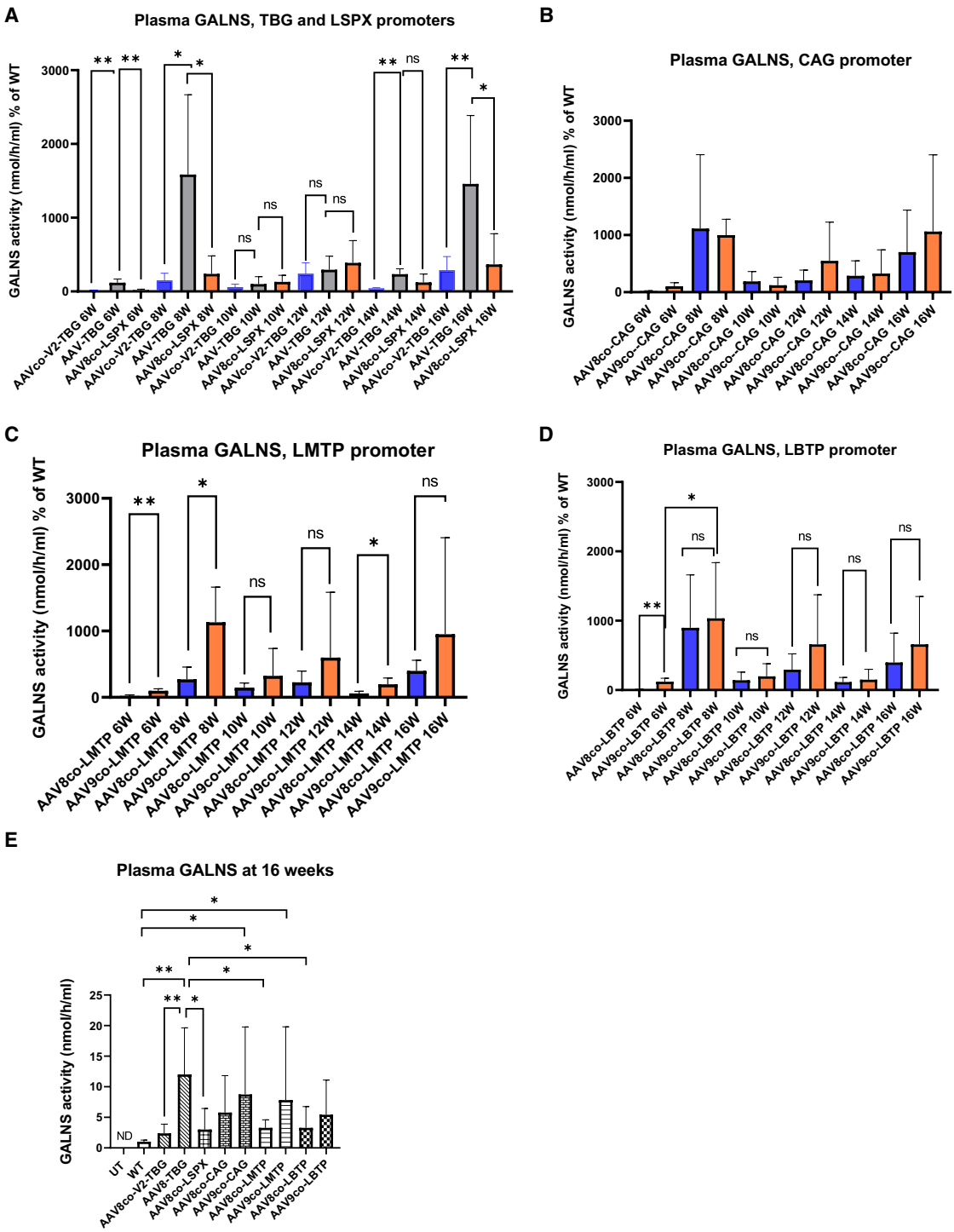

Figure 1. Plasma GALNS activity from 6 weeks through 16 weeks; % of WT

(A) TBG and LSPX promoters; One-way ANOVA for Figure 1A. AAV8-TBG vs. AAV8co-V2-TBG at 14 and 16 weeks (*p <0.05 and **p <0.01, respectively), AAV8-TBG vs. AAV8co-V2-TBG and AAV8co-LSPX not significant at 6, 8, and 12 weeks. (B) CAG promoter; no statistical differences between AAV8co-CAG and AAV9co-CAG at 6, 8, 12, 14, and 16 weeks. AAV9co-LMTP 8 weeks vs. AAV9co-LMTP 6 weeks (t test, *p <0.05). (C) LMTP promoter; no statistical differences between AAV8co-LMTP and AAV9co-LMTP at 6, 8, 10, 12, and 16 weeks. AAV8co-LMTP and AAV9co-LMTP 8 weeks vs. 6 weeks (t test, ***p <0.001 and *p <0.05, respectively). (D) LBTP promoter; No statistical differences between AAV8co-LBTP and AAV9co-LBTP at 6, 8, 10, 12, and 16 weeks. AAV8co-LBTP and AAV9co-LBTP 8 weeks vs. 6 weeks (t test, **p <0.01 and *p <0.05,

(legend continued on next page)

promoter (LBTP), an ApoE enhancer/Osterix (Sp7) bone promoter/hATT liver promoter.

The vectors are being rigorously studied in MPS IVA mice, a species known for its ability to sustain enzyme levels and mitigate skeletal dysplasia. To ensure the comprehensive nature of our research, we have included both male and female mice in each promoter group, aiming to determine whether gender influences the efficacy of gene therapy. This thorough approach to our research instills confidence in the validity of our findings and the potential of gene therapy in treating MPS IVA.

RESULTS

Enzyme activity and KS level in plasma

GALNS enzyme expression in plasma

The findings on GALNS enzyme activity are summarized in Figure 1. GALNS activity in AAV8co-V2-TBG (AAV8 codon-optimized version 2-thyroxin-binding globulin) remained close to wild type (WT) throughout 16 weeks. GALNS activity in AAV8-TBG was significantly higher at 8 weeks, then lowered at weeks 10, 12, and 14 and back to a higher level at 16 weeks. AAV8-TBG activity was significantly higher than AAV8co-V2-TBG at 14 and 16 weeks ($^{*}p$ <0.05 and $^{**}p$ <0.01, respectively). GALNS activity in AAV8co-LSPX was high at 8 and 12 weeks and declined after 14 weeks (Figure 1A).

The plasma GALNS activities in AAV8co-CAG and AAV9co-CAG were significantly higher at 8 weeks than in WT and remained moderately high until 16 weeks (Figure 1B). Plasma GALNS activity in AAV8co-LMTP was close to WT; however, activity in AAV9co-LMTP was significantly higher at 8 weeks than in WT and gradually declined over 16 weeks (Figure 1C). Plasma GALNS activities in AAV8co-LBTP and AAV9co-LBTP were significantly higher at 8 weeks than WT and gradually declined over 16 weeks (Figure 1D). The GALNS activity at 16 weeks old is shown in Figure 1E. Enzyme activities in AAV8-TBG, AAV9co-CAG, and AAV9co-LMTP were significantly higher than in the WT level. Within LMTP and LBTP promoters, enzyme activities in AAV9 vectors were higher than those of the counterpart AAV8 vectors but not significant (Figure 1E). In summary, plasma GALNS activity was expressed in all promoters (liver-specific, CAG, LMTP, and LBTP promoters). However, among liver-specific promoters, AAV8-TBG expressed significantly higher activity than AAV8co-V2-TBG and AAV8co-LSPX. AAV8-TBG also expressed significantly higher activity than AAV8co-LMTP and AAV8co-LBTP. GALNS expression in CAG, LMTP, and LBTP, AAV9co-CAG, AAV9co-LMTP, and AVV9co-LBTP expressed higher GALNS than their counterparts, AAV8 co-CAG, AAV8co-LMTP, and AAV8co-LBTP, respectively.

KS levels in plasma

KS levels in untreated mice were higher throughout the study but were remarkably elevated after 12 weeks. For all promoters, the KS level normalized to the WT level after 6 weeks (Figures 2A–2D). KS levels at 16 weeks old are shown in Figure 2E. KS levels in AAV8co-V2-TBG, AAV8-TBG, AAV8co-LSPX, AAV8co-CAG, AAV9co-CAG, AAV8co-LMTP, AAV9co-LMTP, AAV8co-LBTP, and AAV9co-LBTP were significantly higher than untreated group (Figure 2E). In summary, plasma KS was reduced in all promoters (liver-specific, CAG, LMTP, and LBTP promoters).

GALNS enzyme activity in tissues

GALNS enzyme activity in the liver

The levels of GALNS activity in the liver 12 weeks post intravenous delivery of AAV vectors are shown in Figure 3A. The GALNS activities in all promoters were many-fold higher than in WT. Although not significant, the enzyme activity in AAV8-TBG among the liver-specific promoters was higher than AAV8co-V2-TBG and AAV8co-LSPX. The GALNS activities of AAV9co-CAG, AAV9co-LMTP, and AAV9co-LBTP were higher than those of AAV8-TBG but not significant. The GALNS activity for the AAV9co-LBTP was significantly higher than AAV8co-LBTP ($^{**}p < 0.01$). All promoters expressed higher GALNS activity in the liver than the WT level.

GALNS enzyme activity in muscle

GALNS activity in the muscle was not detected in liver-specific promoters (AAV8co-V2-TBG, AAV8-TBG, and AAV8co-LSPX). Low enzyme activity, comparable to WT, was detected in AAV9co-LBTP (Figure 3B). With the ubiquitous CAG promoter, AAV8co-CAG had significantly ($^{*}p < 0.05$) higher GALNS activity (50 nmol/h/mg) than the WT level. Although not significant, enzyme activity in AAV8co-CAG was also higher than in AAV8co-LMTP (31 nmol/h/mg). AAV9co-LMTP had significantly ($^{*}p < 0.05$) higher activity (73 nmol/h/mg) than WT (Figure 3B). In summary, only CAG and LMTP expressed GALNS activity in the muscle.

GALNS enzyme activity in bone

GALNS activity in bone is shown in Figure 3C. GALNS activities in liver-specific promoters, such as AAV8co-V2-TBG (9.1 nmol/h/mg), AAV8-TBG (5 nmol/h/mg), and AAV8co-LSPX (7.7 nmol/h/mg), were significantly lower than in the WT level (66 nmol/h/mg). The enzyme activities in AAV8co-CAG (95 nmol/h/mg) and AAV9co-LMTP (90 nmol/h/mg) were higher than in the WT level but insignificant. Enzyme activities in AAV9co-CAG (14 nmol/h/mg) and AAV8co-LBTP (13.5 nmol/h/mg) were significantly lower than in the WT level. Enzyme activity in AAV8co-LMTP (26 nmol/h/mg) was also lower than in the WT level. Within the CAG promoter, enzyme activity in AAV8 was significantly ($^{***}p < 0.001$) higher than in AAV9. In LMTP, enzyme activity in AAV9 was also significantly ($^{**}p < 0.01$)

respectively). (E) GALNS activity at 16 weeks, in UT, WT, TBG, LSPX, CAG, LMTP, and LBTP promoters. One-way ANOVA. WT vs. AAV8-TBG ($^{**}p < 0.01$), AAV9co-CAG, and AAV9co-LMTP ($^{*}p$ <0.05). AAV8-TBG vs. AAV8co-V2-TBG ($^{**}p < 0.01$), AAV8co-LSPX ($^{*}p$ <0.05), AAV8co-LMTP ($^{*}p$ <0.05), and AAV8co-LBTP ($^{*}p$ <0.05). UT, untreated; WT, wild-type; TBG, thyroxin-binding globulin; LSPX, human alpha1-antitrypsin (hAAT); CAG, ubiquitous cytomegalovirus early enhancer/chicken β-actin; LMTP, liver-muscle tandem promoter; and LBTP, liver-bone tandem promoter.

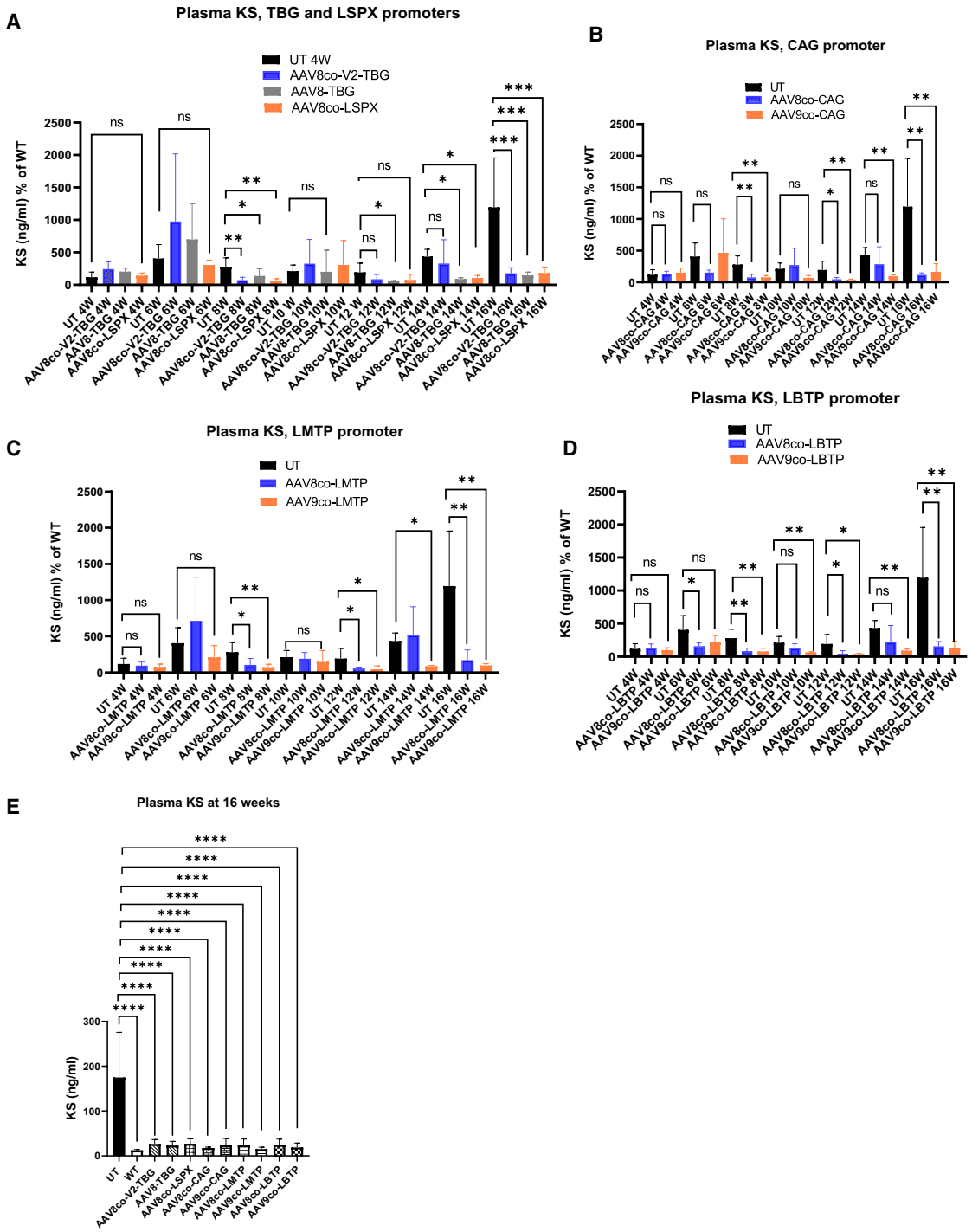

Figure 2. Plasma KS levels from 6 weeks through 16 weeks; % of WT

(A) TBG, and LSPX promoters. One-way ANOVA. No statistical differences between UT vs. AAV8co-V2-TBG, AAV8-TBG, and AAV8co-LSPX at weeks 4, 6, and 10. Week 8, UT vs. AAV8co-V2-TBG, AAV8co-LSPX, and AAV8-TBG (**$p < 0.01$ and *$p < 0.05$, respectively). Week 12, UT vs. AAV8-TBG (*$p < 0.05$). Week 14, UT vs. AAV8-TBG and AAV8co-LSPX KS (*$p < 0.05$). Week 16, UT vs. AAV8co-V2-TBG, AAV8-TBG, and AAV8co-LSPX (***$p < 0.001$). (B) CAG promoter; one-way ANOVA. Weeks 4, 6, and 10 had no statistical differences, UT vs. AAV8co-CAG and AAV9co-CAG. Week 8, UT vs. AAV8co-CAG and AAV9co-CAG (**$p < 0.01$). Week 12, UT vs. AAV8co-CAG and AAV9co-CAG (*$p < 0.05$ and **$p < 0.01$, respectively). Week 14, UT vs. AAV9co-CAG (**$p < 0.01$). Week 16, UT vs. AAV8co-CAG and AAV9co-CAG (**$p < 0.01$). (C) LMTP promoter; one-way ANOVA. Weeks 4, 6, and 10 had no significant change, UT vs. AAV8co-LMTP and AAV9co-LMTP. Week 8, UT vs. AAV8co-CAG and

(legend continued on next page)

higher than in AAV8. Enzyme activity in AAV8co-CAG was also significantly (****$p < 0.0001$) higher than in AAV8co-LBTP. Overall, enzyme activity in liver-specific promoters was lower in bone than in LMTP, LBTP, and CAG promoters.

GALNS enzyme activity in the trachea

GALNS enzyme activity in the trachea is shown in Figure 3D. All groups had lower GALNS activity than WT (95 nmol/h/mg). However, the enzyme activity in AAV8co-CAG was higher (12 nmol/h/mg) than liver-specific promoters (AAV8co-V2-TBG, AAV8-TBG, and AAV8co-LSPX) and LBTP (AAV8co-LBTP and AAV9co-LBTP). Moreover, enzyme activity in AAV8co-CAG was also higher than in AAV9co-CAG. Although not significant, enzyme activity in AAV9co-LMTP was higher than that of its counterpart, AAV8. Overall, none of the promoters achieved the WT level. This is because the trachea is an avascular tissue and is hard to penetrate. Therefore, the enzymes could not be taken up efficiently by tracheal chondrocytes.

GALNS enzyme activity in the heart

Heart GALNS activity is shown in Figure 3E. All liver-specific promoters had lower enzyme activity than WT (0.63 nmol/h/mg). GALNS activity in AAV8co-CAG (13 nmol/h/mg), AAV8co-LMTP (15 nmol/h/mg), and AAV9co-LMTP (11 nmol/h/mg) was significantly higher than WT (****$p < 0.0001$). Within the CAG group, enzyme activity in the AAV8 serotype was significantly higher than in its counterpart, AAV9 (****$p < 0.0001$). AAV8co-LMTP also had higher activity than AAV9co-LMTP, although not significant. Enzyme activity in LBTP was low, close to WT levels. Overall, LMTP expressed the highest GALNS enzyme in skeletal and cardiac muscle.

GALNS enzyme activity in spleen

All groups had higher enzyme activity than WT (10 nmol/h/mg) (Figure 3F). Enzyme activities in CAG promoters (AAV8co-CAG and AAV9co-CAG) were 22 nmol/h/mg and 14 nmol/h/mg, respectively. Enzyme activities in liver-specific promoters (AAV8co-V2-TBG, AAV8-TBG, and AAV8co-LSPX) were 13, 18, and 13 nmol/h/mg, respectively. Enzyme activities in AAV8co-LMTP and AAV9co-LMTP were 13 and 17 nmol/h/mg, respectively. GALNS activities in AAV8co-LBTP and AAV9co-LBTP were 15 and 18 nmol/h/mg, respectively.

KS levels in tissues

KS level in liver

There was a significant difference in liver KS levels between the WT and untreated groups. The liver KS levels in untreated mice were significantly higher than in treated mice (Figure 4A). The KS levels in liver-specific AAV8-TBG and AAV9co-LMTP were normalized entirely to the WT KS level. The KS levels in all other treated groups were normalized close to WT levels.

KS level in muscle

The KS levels in the muscle are shown in Figure 4B. There was no difference in muscle KS levels between WT and untreated groups. Liver-specific promoters did not show a change in KS level. However, AAV8co-LSPX had reduced KS levels when compared with the untreated group. In the CAG group, the KS level of only AAV8co-CAG was reduced when compared with untreated mice. Moreover, in LMTP, the KS level of AAV9co-LMTP was significantly (*$p < 0.05$) reduced when compared with untreated mice. The KS level of LBTP was also reduced but comparatively to a lower extent than the other decreasing groups. Thus, GALNS expression in LMTP provided a lower KS level in the muscle.

KS level in bone

There was a significant difference in bone KS levels between WT and untreated groups. Bone KS levels in all treated mice were significantly lower than in untreated mice (Figure 4C). KS levels in AAV8co-LSPX, CAG, and LMTP promoters were reduced below the WT levels. KS levels in liver-specific promoters (AAV8co-V2-TBG and AAV8-TBG) and LBTP (AAV8co-LBTP and AAV9co-LBTP) were normalized to WT levels. GALNS expression in LBTP was low (also low copy number); however, the KS level was reduced, as seen in all other promoters.

Biodistribution of AAV genome

Genome copies of AAV vectors in liver, muscle, and bone were quantified by digital PCR as described in the materials and methods section. In the liver, all AAV vectors were found in abundance (Figure S1A) and significantly higher than untreated mice. The copy numbers in muscle were significantly higher in AAV9co-LMTP and AAV9co-LBTP than in the WT level (Figure S1B). Genome copy numbers in AAV8co-LSPX, AAV8co-CAG, and AAV9co-LMTP were significantly higher in bone than in untreated mice (Figure S1C). Overall, the copy numbers in muscle and bone were significantly lower than in the liver.

Treated mice expressed anti-hGALNS antibodies in plasma

To check humoral response against GALNS, an enzyme-linked immunosorbent assay (ELISA) was performed using plasma from WT, untreated, and treated mice. All treated groups showed significantly higher levels of circulating anti-hGALNS antibodies than

AAV9co-CAG (*$p < 0.05$ and **$p < 0.01$, respectively). Week 12, UT vs. AAV8co-CAG and AAV9co-CAG (*$p < 0.05$). Week 14, UT vs. AAV9co-CAG (*$p < 0.05$). Week 16, UT vs. AAV8co-CAG and AAV9co-CAG (**$p < 0.01$). (D) LBTP promoter; one-way ANOVA. In Week 4, there was no significant change in UT compared with AAV8co-LBTP and AAV9co-LBTP. Week 6, UT vs. AAV8co-LBTP (*$p < 0.05$). Week 8, UT vs. AAV8co-LBTP and AAV9co-LBTP (**$p < 0.01$). Weeks 10 and 14, UT vs. AAV9co-LBTP (**$p < 0.01$). Weeks 12 and 16, UT vs. AAV8co-LBTP and AAV9co-LBTP (*$p < 0.05$ and **$p < 0.01$, respectively). (E) KS levels at 16 weeks, in WT, TBG, LSPX, CAG, LMTP, and LBTP promoters. One-way ANOVA. UT vs. WT, AAV8co-V2-TBG, AAV8-TBG, AAV8co-LSPX, AAV8co-CAG, AAV9co-CAG, AAV8co-LMTP, AAV9co-LMTP, AAV8co-LBTP, and AAV9co-LBTP (****$p < 0.0001$). UT, untreated; WT, wild-type; TBG, thyroxin-binding globulin; LSPX, human alpha1-antitrypsin (hAAT); CAG, ubiquitous cytomegalovirus early enhancer/chicken β-actin; LMTP, liver-muscle tandem promoter; and LBTP, liver-bone tandem promoter.

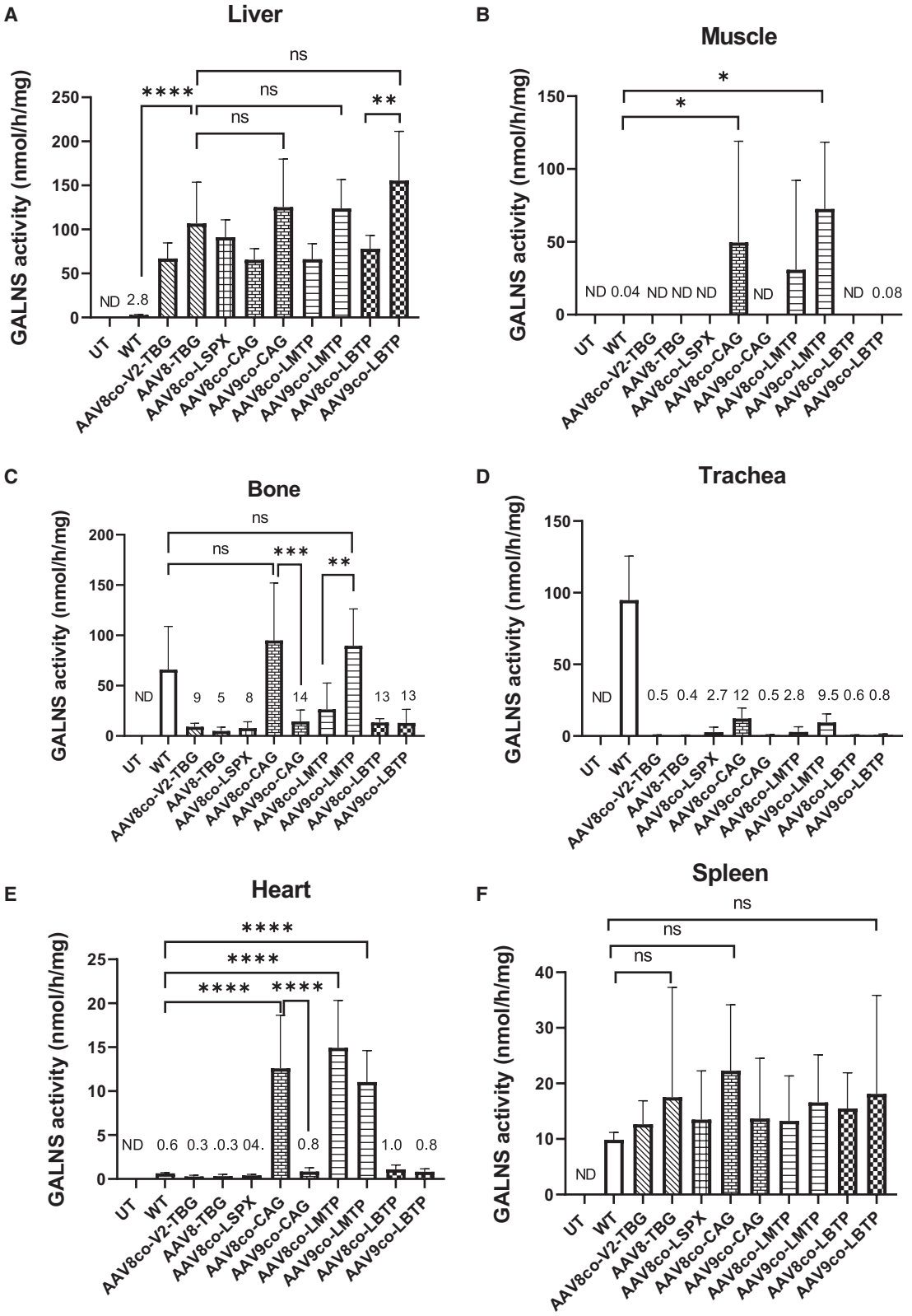

(legend on next page)

untreated mice (Figure 5), identified in the previous reports.[19,21] The AAV9 vectors in LMTP and LBTP were higher responses to anti-GALNS antibodies. In general, the level of anti-GALNS antibodies was higher in female mice than in male mice in all groups. The data presented here are a combined value of male and female mice in each group.

Micro-computed tomography analysis of femur

Micro-computed tomography (micro-CT) analysis of mice femurs was performed. Trabecular bone morphometry is shown in Figures 6A–6C. Trabecular bone volumes in most groups were lower than in untreated mice but similar to or higher than in WT mice. In addition, AAV8co-V2-TBG and AAV8co-LMTP were significantly lower than the untreated mice group (Figures 6A and 6D). Within LMTP, the AAV8 serotype was lower than AAV9. In addition, AAV8co-V2-TBG was significantly lower than AAV8co-LSPX. Trabecular numbers in all vectors except (AAV8co-V2-TBG and AAV8co-LMTP) were similar or higher than in WT mice but lower than in untreated mice. AAV8co-V2-TBG and AAV8co-LMTP were significantly lower than the untreated group. In addition, although not significant, CAG and LBTP promoter AAV9 vectors had higher trabecular numbers than their counterpart AAV8 vectors. However, AAV9co-LMTP had a significantly higher number than AAV8co-LMTP. Bone mineral density (BMD) was lower in all treated groups than in the untreated group (only AAV8co-V2-TBG and AAV8co-LMTP were significant). Within the liver-specific group, AAV8co-V2-TBG had significantly lower BMD than AAV8-TGB and AAV8co-LSXP. Moreover, in trabecular bone, bone volume fraction (%) (BV/TV; bone volume/total volume [bone + other tissues]) of treated knockout (KO) mice was reduced compared with untreated KO mice (Figure 6D). The maximum reduction in the percentage of BV/TV was found in AAV8co-LMTP.

The cortical bone architecture was analyzed and is shown in Figures S2A–S2C. Cortical bone areas in AAV8co-V2-TBG, AAV9co-CAG, and AAV8co-LMTP were significantly lower than in untreated mice. Within LMTP, the AAV9 vector was significantly higher than AAV8 (Figure S2A). The medullary areas of AAV9co-LBTP were significantly higher than those in the untreated group (Figure S2B). Within the LBTP group, the AAV9 medullary area was significantly higher than AAV8. Most vectors had slightly higher or similar medullary area than the untreated group (Figure S2B). Cortical tissue mineral density (TMD) in AAV8co-V2-TBG, AAV8co-LSPX, AAV8co-LMTP, AAV9co-LMTP, and AAV8co-LBTP was significantly higher than the untreated group. In addition, LBTPco-AAV9 TMD was significantly higher than LBTPco-AAV8 (Figure S2C). However, no significant change was seen in female mice in cortical bone and medullary areas, as shown in Figures S2D and S2E. TMD was significantly lower in WT and AAV9co-LBTP (Figure S2F).

Bone and cartilage pathology

Effects of the AAV vector on femurs and tibias of MPS IVA mice were assessed 12 weeks post-injection. The untreated group of mice exhibited excessive GAG storage vacuoles in the growth plates of tibias (Figure 7A), articular cartilage (Figure 7B), meniscus, and ligaments. Growth plates also exhibited disorganized column structures with vacuolated chondrocytes (Figures 7A and 7B). In treated groups (TBG, CAG, LMTP, and LBTP), growth plates, articular cartilage, ligaments, and meniscuses of the knee joint had a partial reduction of storage material, and the column structure of chondrocytes was improved but remained disorganized and distorted.

The chondrocyte cell size was measured to evaluate the improvement of vacuolization in cartilage cells of the growth plate. Chondrocyte cell size was significantly reduced in growth plate lesions, including femurs and tibias of treated groups (TBG, CAG, LMTP, and LBTP), compared with untreated mice (Figures 7C and 7D). Moreover, we assessed the amelioration of vacuoles and disorganized column structures in MPS IVA mice as pathological scores, which moderately improved in treated mouse groups with each AAV vector compared with untreated mice. Pathological scoring of mice treated with LMTP was markedly lower in particular discs and ligaments than in other groups (TGB, CAG, and LBTP) (Figures 8A–8D). These results suggested that the impact of the LMTP promoter construct on the bone lesions of MPS IVA mice was greater than that of other promoters (TGB, CAG, and LBTP).

Untreated MPS IVA mice exhibited GAG storage vacuoles in heart valves and muscles. AAV8co-V2-TBG, AAV8co-LSPX, and AAV8co-CAG provided clearance of vacuoles (Figure S3). AAV8co-LMTP and AAV9co-LMTP provided nearly complete clearance in these heart lesions of treated mice (Figure S3).

DISCUSSION

Our previous study showcased the potential of AAV gene therapy in MPS IVA mice, demonstrating a significant reduction in storage materials in the articular cartilage and growth plate region. While this did not completely restore skeletal lesions, it did provide a promising foundation for further research.[19] In the present study, we tested nine different AAV vectors expressing hGALNS under the control of a liver-specific TBG or LSPX promoter, a ubiquitous promoter

Figure 3. GALNS activity in tissues

Liver (A), muscle (B), bone (C), trachea (D), heart (E), and spleen (F). One-way ANOVA. Liver; WT vs. AAV8-TBG (****$p < 0.0001$), AAV8-TBG vs. AAV9co-CAG, AAV9co-LMTP, and AAV9co-LBTP not significant. AAV8co-LBTP vs. AAV9co-LBTP (**$p < 0.01$). Muscle; WT vs. AAV8co-CAG and AAV9-co-LMTP (*$p < 0.05$). Bone; WT vs. AAV8co-CAG and AAVco-LMTP not significant, AAV8co-CAG vs. AAV9co-CAG (***$p < 0.001$), AAV9co-LMTP vs. AAV8co-LMTP (**$p < 0.01$). Trachea; no significance. Heart; WT vs. AAV8co-CAG, AAV8co-LMTP, and AAV9co-LMTP (****$p < 0.0001$), AAV8co-CAG vs. AAV9co-CAG (****$p < 0.0001$). Spleen; WT vs. AAV8-TBG, AAV8co-CAG, AAV9co-LBTP non-significant. WT, wild-type; TBG, thyroxin-binding globulin; CAG, ubiquitous cytomegalovirus early enhancer/chicken β-actin; LMTP, liver-muscle tandem promoter; and LBTP, liver-bone tandem promoter.

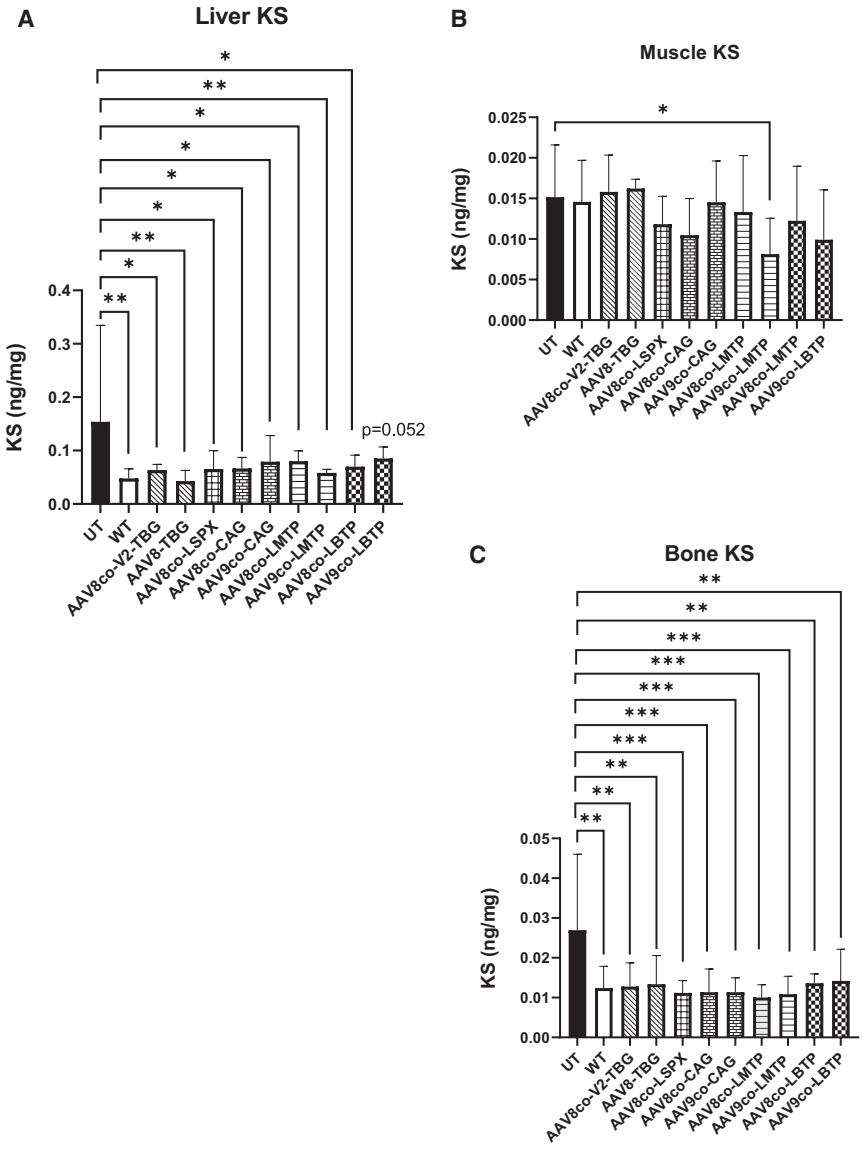

Figure 4. KS level in tissues

Liver (A), muscle (B), and bone (C). One-way ANOVA. Liver; UT vs. WT, AAV8-TBG, and AAV9co-LMTP (**p < 0.01), UT vs. AAV8co-V2-TBG, AAV8co-LSPX, AAV8co-CAG, AAV9co-CAG, AAV8co-LMTP, and AAV8co-LBTP (*p < 0.05). Muscle; UT vs. AAV9co-LMTP (*p < 0.05). Bone; UT vs. WT, AAV8co-V2-TBG, AAV8-TBG, AAV8co-LBTP, and AAV9co-LBTP (**p < 0.01), UT vs. AAV8co-LSPX, AAV8co-CAG, AAV9co-CAG, AAV8co-LMTP, and AAV9co-LMTP (***p < 0.001). UT, untreated; WT, wild-type; TBG, thyroxin-binding globulin; LSPX, human alpha1-antitrypsin (hAAT); CAG, ubiquitous cytomegalovirus early enhancer/chicken β-actin; LMTP, liver-muscle tandem promoter; and LBTP, liver-bone tandem promoter.

(CAG), an LMTP, or an LBTP to determine the most effective treatment on bone lesions in MPS IVA mice.

The GALNS enzyme activity in plasma was elevated in every treated group; however, TBG and CAG promoters with AAV8 provided higher levels than AAV8co-LMTP and AAV8co-LBTP. Conversely, AAV9co-LMTP and AAV9co-LBTP had enzyme levels similar to those of TBG and CAG promoters. We used LMTP and LBTP along with liver-specific promoters and found supraphysiological enzyme activity levels in the liver from all groups; however, the AAV9 serotype was more effective in CAG, LMTP, and LBTP promoters than the AAV8 serotype. Thus, the expression of AAV vectors in the liver reflects the level of GALNS in plasma. The GALNS enzyme activity in muscle was substantially detectable in CAG (AAV8) and LMTP (AAV8 and AAV9), while almost no enzyme activity was found in the WT mice. Notably, only CAG (AAV8) and LMTP (AAV9) provided supraphysiological levels of enzyme activity in bone. The AAV9co-LMTP produced higher enzyme activity in bone and muscle than the other promoters. It is interesting to observe that bone KS levels were normalized to WT levels in all promoters despite the enzyme activity level. KS levels in bone (femur in this study) reflect four types of bone cells (osteoblasts, osteoclasts, osteocytes, and osteoprogenitor [or osteogenic] cells), chondrocytes, and extracellular matrix, where KS is synthesized and/or used as part of structural components, proteoglycans like aggrecan. The avascular growth plate region, which is hard-to-reach tissue, is a tiny portion. Therefore, we hypothesize that normalization of bone KS level results from accessible bone cells but not from the chondrocytes in the growth plate and that a small amount of enzyme may be required to deliver to the bone to reduce KS in bone cells but not for the chondrocytes. This finding could also explain why the pathology in chondrocytes of the growth plate is partially corrected in this study despite the KS normalization of the whole femur.

The optimal AAV vector constructs for bone and cartilage lesions of MPS IVA remain unknown; therefore, we evaluated micro-CT analysis for MPS IVA mice to assess therapeutic efficacy from single and tandem promoters using AAV8 and AAV9 serotypes. In most groups, trabecular bone volume, number, and BMD were lower than those in the untreated mice group.

Recombinant AAV vectors are under intensive investigation in many clinical trials after emerging as highly promising vectors for human gene therapy. Exemplifying their power and potential is the authorization of six gene therapy products based on WT AAV serotypes: Glybera (AAV1), Luxturna (AAV2), and most recently, Zolgensma

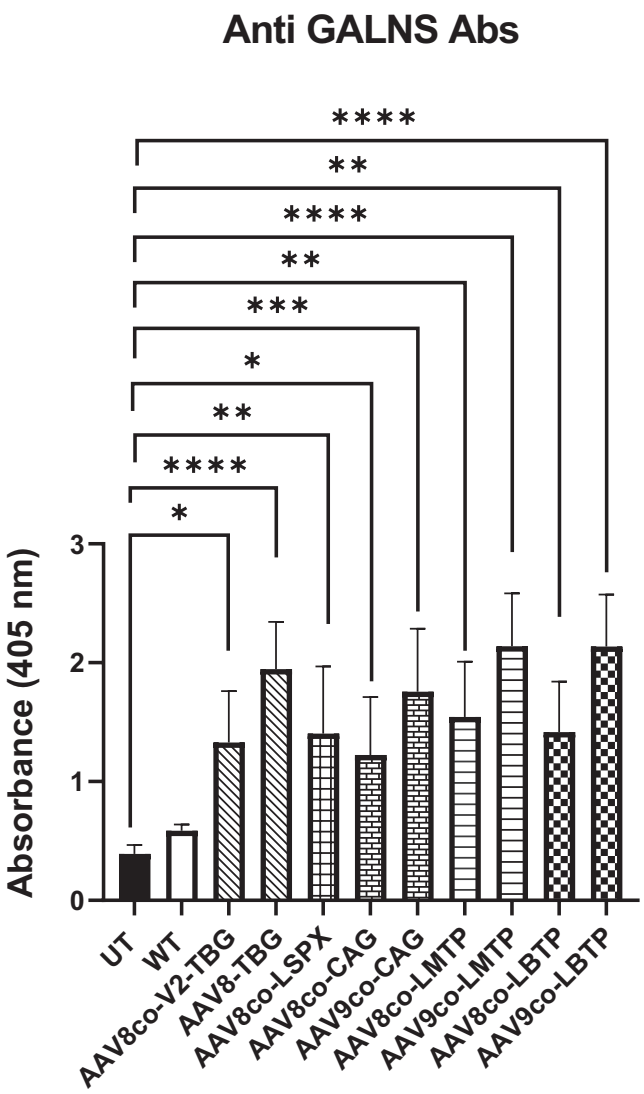

Figure 5. Detection of GALNS antibodies

Detection of GALNS antibodies by ELISA in UT, WT, TBG, LSPX, CAG, LMTP, and LBTP promoters. UT vs. AAV8co-V2-TBG, AAV8co-CAG (*$p < 0.05$), UT vs. AAV8co-LSPX, AAV8co-LMTP, and AAV8co-LBTP (**$p < 0.01$), UT vs. AAV9co-CAG (***$p < 0.001$), UT vs. AAV8-TBG, AAV9co-LMTP, and AAV9co-LBTP (****$p < 0.0001$). UT, untreated; WT, wild-type; TBG, thyroxin-binding globulin; LSPX, human alpha1-antitrypsin (hAAT); CAG, ubiquitous cytomegalovirus early enhancer/chicken β-actin; LMTP, liver-muscle tandem promoter; and LBTP, liver-bone tandem promoter.

(AAV9),[22] Valoctocogene roxaparvovec (AAV5) for hemophilia A,[23] and AAV8, AAV9, and lentiviral vectors for hemophilia B.[24] The number of clinical trials of AAV-based gene therapies is on the rise, and as of 2022, more than 200 trials have been conducted.[25] In the MPS field, TBG promoter has been reported to improve bone length in MPS VI feline and rat models,[26,27] leading to ongoing clinical trials for MPS VI using a liver-specific promoter construct packaged into AAV8 (NCT03173521).[28] Wood and Bigger summarize the gene therapy clinical trials for MPS.[29] CAG promoters have been used in AAV gene therapy clinical trials for MPS I, II, and IIIA with various routes of administration, showing therapeutic effects (NCT03580083, NCT03566043, NCT03612869).

Colella et al. have made significant strides in validating the AAV gene therapeutic approach with the tandem promoter in infantile mice with Pompe disease.[30] This disease, caused by a lack of the acid-alpha-glucosidase (GAA) enzyme, presents a significant challenge for gene therapy. However, the efficient tandem promoter has shown promise in preventing immune responses to GAA following systemic AAV gene transfer in immunocompetent Gaa−/− newborn mice. This work demonstrates that neonatal gene therapy with either AAV8 or AAV9 in Gaa−/− mice can lead to persistent therapeutic efficacy when using an LMTP that provides high and persistent transgene expression in non-dividing extra-hepatic tissues. The authors' conclusion that the tandem promoter can overcome critical limitations of AAV gene therapy is a hope for treating pediatric conditions requiring persistent multi-systemic transgene expression and prevention of anti-transgene immunity. Nieuwenhuis et al. reported the AAV1 vector in four commonly used promoters: the short CMV early enhancer/chicken β-actin (sCAG), human cytomegalovirus (hCMV), mouse phosphoglycerate kinase (mPGK), and human synapsin (hSYN) promoters. The mPGK and hSYN promoters directed the most robust transgene expression.[31] The mPGK promoter did drive expression in cortical neurons and oligodendrocytes. In contrast, transduction with AAV harboring the hSYN promoter resulted in neuron-specific expression, including perineuronal net expressing interneurons and layer V corticospinal neurons. This promoter comparison study improves transgene delivery into the brain and spinal cord.[31] In another study, Nieuwenhuis et al. reported five promoters (chicken β-actin [CBA], CMV, sCAG, mPGK, and hSYN) in AAV2 for gene delivery.[32] AAV2 is commonly used to deliver transgenes to retinal ganglion cells via intravitreal injection. The promoters driving enhanced green fluorescent protein (eGFP) were examined in adult C57BL/6J mice eyes and tissues of the visual system. The eGFP expression was most robust in the retina, optic nerves, and brain when driven by the sCAG and SYN promoters. By comparison, CBA, CMV, and PGK had moderate expression.[32] Yang et al. showed that different AAV serotypes had different transduction efficiencies in bone cells, including osteoblasts and chondrogenic cells.[33] Chen et al. showed that intra-articular injection of AAV2 provided high transduction efficiencies in chondrocytes located in the deep layer of the articular cartilage.[34]

Despite the significant advancement of AAV gene therapy, it has also become evident that the current AAV vector generation will require improvements in transduction potency, antibody evasion, and cell/tissue specificity to allow lower and safer vector doses.[35] Therefore, further studies should optimize the administration route of AAV vectors and AAV serotypes for bone and cartilage lesions in MPS IVA mice and relevant larger animal models.[19,21] Bertolin et al. (2021) demonstrated the therapeutic effects on MPS IVA rats with AAV9-*Galns*, resulting in widespread transduction of bones, cartilage, and

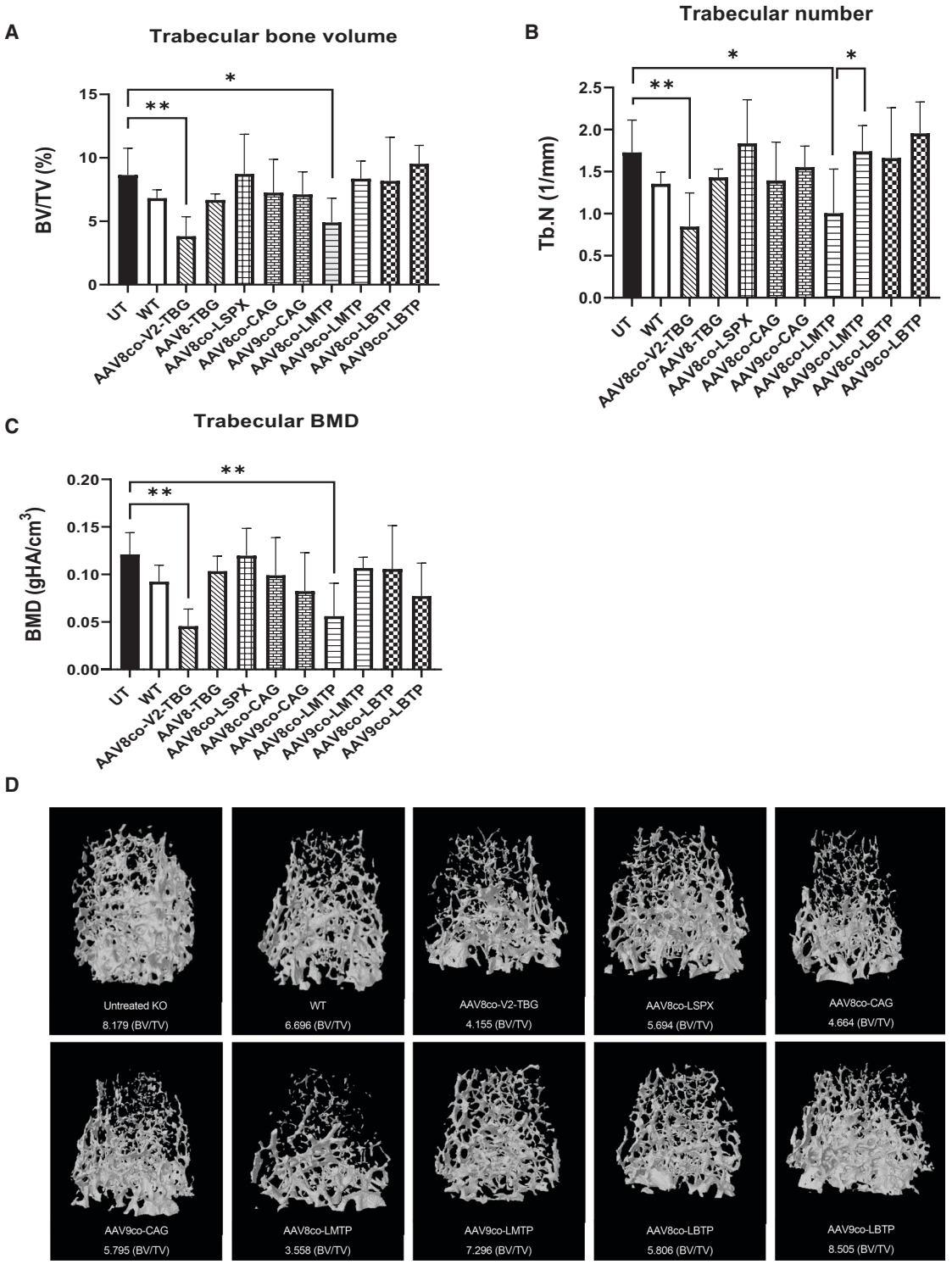

Figure 6. Trabecular bone morphometry

Trabecular bone volume fraction (A), trabecular number (B), trabecular BMD (C), trabecular bone structure (BV/TV) of male mice, UT, WT, liver-specific (AAV8co-V2-TBG and AAV8co-LSPX) promoters, CAG, LMTP, LBTP promoters. (D) One-way ANOVA, trabecular bone volume fraction; UT vs. AAV8co-V2-TBG (**$p < 0.01$) and

(legend continued on next page)

peripheral tissues and successive improvement in skeletal and non-skeletal lesions. This study suggested the potential of AAV gene therapy for MPS IVA; however, the rat (but not human) *Galns* cDNA with AAV9 vector was used, and immunogenicity due to the species difference was eliminated. Therefore, it remained unknown whether human *GALNS* cDNA with the AAV vector provides the same efficacy in different species like mice or rats, which we investigated here.[36] Since no vector in this study can completely correct bone pathology, we may need a humanoid mouse or rat model to show the more therapeutic effects of human *GALNS* cDNA. We will also consider administering the higher dose, which could be toxic for mice and may be tough to use for human clinical trials. Since bone pathology in MPS IVA mice (avascular growth plate region and ligaments) is progressive and challenging to reverse, we plan to administer AAV vectors to newborns. Another way is to eliminate immune reaction against the gene product (GALNS). We are investigating the immune-tolerant induction against the gene product into the MPS IVA mice before AAV gene therapy.

In conclusion, intravenous administration of the AAV9 vector with an LMTP promoter led to more therapeutic potential for treating MPS IVA bone and cartilage lesions. This preclinical study provides valuable information on promoter selection for AAV-mediated gene therapy for human patients with MPS IVA. Further studies are required to understand and circumvent observed challenges posed by the immune responses against the expressed enzyme and the AAV vector to successfully translate this approach to the clinic.

MATERIALS AND METHODS

Cassette design and expression of AAV vector production

AAV8 vectors expressing codon-optimized *hGALNS* under the control of TBG (AAV8-TBG-*hGALNS*co-V2, AAV8-TBG-*hGALNS*, or AAV8co-LSPX), AAV8 and AAV9 vectors expressing codon-optimized *hGALNS* with (CAG) promoter (AAV8co-CAG-*hGALNS*, AAV9co-CAG-*hGALNS*), LMTP (AAV8co-LMTP-*hGALNS*, AA V9co-LMTP-*hGALNS*), and LBTP (AAV8co-LBTP-*hGALNS*, AA V9co-LBTP-*hGALNS*) were produced by Vector Core of Regenxbio Inc.

In the text, we referred to specific TBG promoters (AAV8-TGB-*hGALNS* [AAV8-TGB] and AAV8co-V2-TGB-*hGALNS* [AAV8co-V2-TBG]) as AAV8-TGB and AAV8co-V2-TGB (version2; depleting CG dinucleotides plus codons optimized), respectively; to liver-specific promoter with modification of human alpha 1-antitrypsin (hAAT) as AAV8co-LSPX; ubiquitous CAG promoters (AAV8co-V2-CAG-*hGALNS* and AAV9co-V2-CAG-*hGALNS*) as AAV8co-CAG and AAV9co-CAG, respectively; LMTP (AAV8co-V2-LMTP-*hGALNS* and AAV9co-V2-LMTP-*hGALNS*) as AAV8co-LMTP and AAV9co-LMTP, respectively; and to LBTP (AAV8co-V2-LBTP-*hGALNS* and AAV9co-V2-LBTP-*hGALNS*) as AAV8co-LBTP and AAV9co-LBTP. These vectors were transfected in a human liver cell line, Huh-7 cells, and determined the activity levels in both cell lysate and supernatant 48 h post-transfection.

Animal experimentation

We have used *Galns* KO (*Galns*$^{-/-}$) MPS IVA mouse models with the C57BL/6 background. The KO mice had no detectable GALNS enzymatic activity in blood and tissues and displayed the excessive accumulation of storage materials primarily within reticuloendothelial Kupffer cells, muscle, heart valves, and chondrocytes, including articular cartilage and growth plate.[37] Homozygous male and female MPS IVA mice at 4 weeks of age were treated with nine different AAV vectors with a dose of 5×10^{13} genome copies (GC)/kg via the lateral tail veins with TBG promoters (AAV8co-V2-TBG and AAV8-TBG), AAV8co-LSPX promoter, AAV8 and AAV9 vectors with the CAG promoter (AAV8co-CAG and AAV9co-CAG), LMTP (AAV8co-LMTP and AAV9co-LMTP), and LBTP (AAV8co-LBTP and AAV9co-LBTP).

Another cohort of MPS IVA KO mice was administered with phosphate-buffered saline (PBS) (untreated group). The WT mouse group was also treated with PBS. The total dose volume administration was approximately 100 μL per mouse. Each group had six mice (three males and three females). Approximately 100 μL of blood was collected in tubes with EDTA (Becton Dickinson, Franklin Lakes, NJ) every other week from all animals in the study. The blood was centrifuged at 8,000 rpm for 10 min, and the separated plasma was kept at −20°C until the GALNS enzyme assay and GAG assay were performed. At 16 weeks, mice were euthanized in a CO_2 chamber and perfused with 20 mL of 0.9% saline. Liver, heart, lung, muscle, trachea, spleen, kidney, and knee joints were collected and stored at −80°C until processing for the GALNS enzyme assay and GAG assay. In addition, knee joint samples were collected and stored in 10% neutral buffered formalin for histopathology analysis. All animal care and procedures followed NIH guidelines and were approved by the Nemours Institutional Animal Care and Use Committee.

GALNS enzyme activity assay

Adeno-associated viruses can have specific tropism for specific organs and tissues of the body depending on their serotype. As mentioned above, AAV8 is best known for its strong tropism to liver cells in different models, including murine, canine, and non-human primates (NHPs).[35,38–45] Adeno-associated virus 8 (AAV8) was also found to be the most efficient for the transduction of both skeletal and cardiac muscles.[46] However, AAV9 transduction efficiency in most tissues is superior to other AAVs.[47,48] Moreover, the CNS of murine, NHP, and feline models has a unique feature compared with other serotypes.[49–53] In some cases, transduction of AAV9 is five- to 10-fold

AAV8co-LMTP (*$p < 0.05$). Trabecular number; UT vs. AAV8co-V2-TBG (**$p < 0.01$) and AAV8co-LMTP (*$p < 0.05$), AAV8co-LMTP vs. AAV9co-LMTP (*$p < 0.05$). Trabecular BMD; UT vs. AAV8co-V2-TBG and AAV8co-LMTP (**$p < 0.01$). BMD, bone mineral density; UT, untreated; WT, wild-type; TBG, thyroxin-binding globulin; LSPX, human alpha1-antitrypsin (hAAT); CAG, ubiquitous cytomegalovirus early enhancer/chicken β-actin; LMTP, liver-muscle tandem promoter; and LBTP, liver-bone tandem promoter.

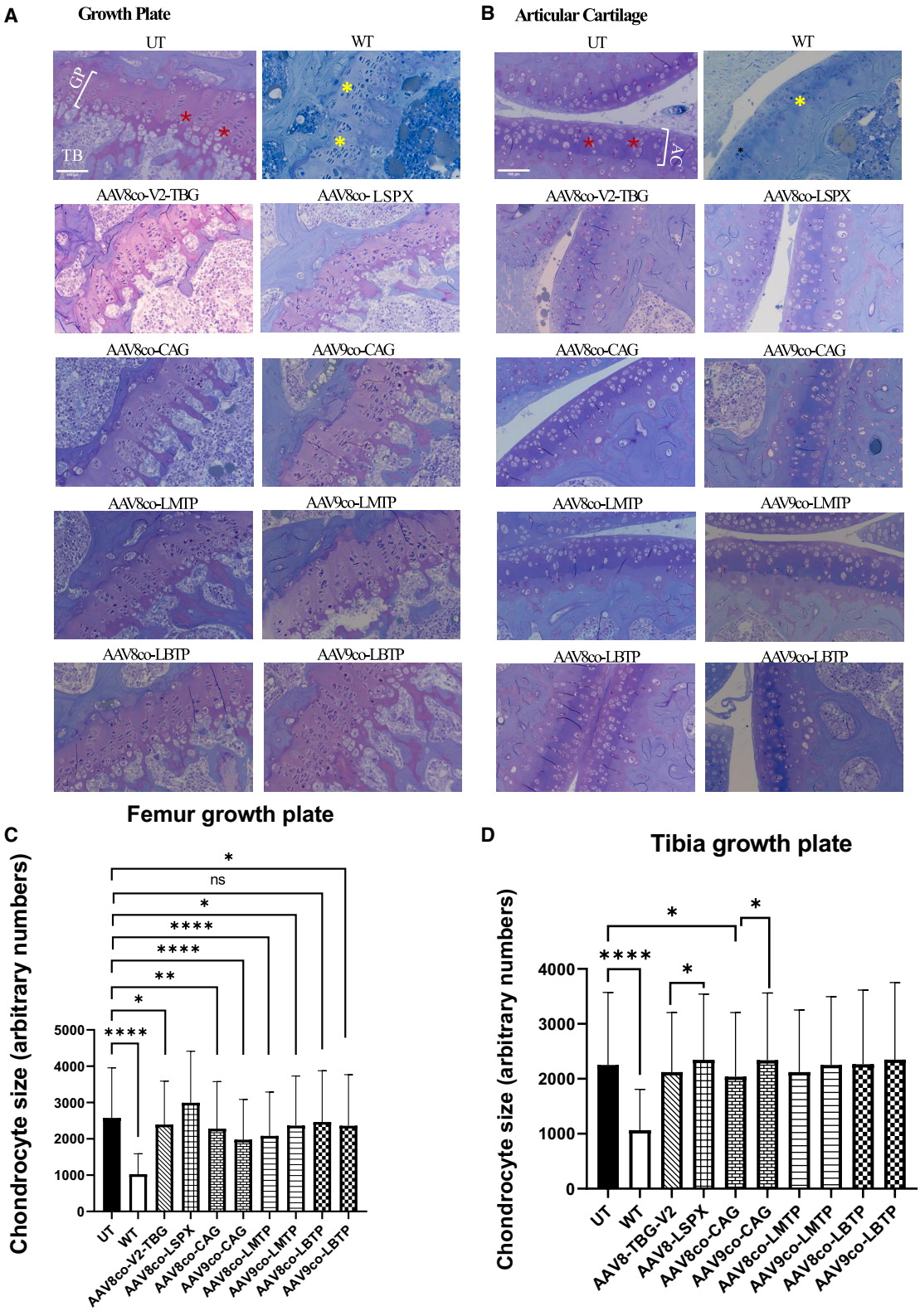

(legend on next page)

higher than AAV8 for murine, NHP, and porcine cardiac muscle.[24,54–58] Another study showed that AAV9 is superior to other AAVs with robust transduction of murine hepatocytes, skeletal muscles, and pancreatic cells.[58] Therefore, we used both AAV8 and AAV9 vectors in ubiquitous CAG promoter, LMTP, and LBTP. We also used liver-specific TBG and liver-specific LSPX promoters. In addition, we used codon-optimized GALNS to maximize GALNS enzyme production. We used different promoters to evaluate which promoter facilitates the highest expression of GALNS enzyme in plasma and tissue and the correction of accumulated GAGs and bone pathology. These vectors were delivered intravenously into 4-week-old MPS IVA knockout (KO) mice at a dose of 5×10^{13} GC/kg. Blood samples were collected every other week to analyze the enzyme activity and KS levels. After 12 weeks post-injection at necropsy, tissue samples were taken from different organs for GALNS activity and KS levels. Knee joints and heart valves were used for histopathology analysis.

GALNS activity in plasma and tissues was determined as described.[19] Frozen tissues were homogenized with a homogenization buffer containing 25 mM Tris-HCl (pH 7.2) and 1 mM phenylmethylsulfonyl fluoride using an Omni Bead Ruptor Bead Mill Homogenizer (OMNI International, Kennesaw, GA) according to manufacturer recommendations for speed and time. Tissue homogenate was transferred to a 1.5-mL tube and centrifuged for 30 min at 12,000 × *g*, at 4°C. The clear supernatant was used for enzyme activity, as shown below.

Plasma or tissue lysate and 22 mM 4-methylumbelliferyl-β-galactopyranoside-6-sulfate (Carbosynth, San Diego, CA) in 0.1 M NaCl/0.1 M sodium acetate (pH 4.3) were incubated in a HEIDOLPH Incubator (Grainger, Lake Forest, IL) at 37°C for 17 h. Then, 10 mg/mL β-galactosidase from *Aspergillus oryzae* (Sigma-Aldrich, St. Louis, MO) in 0.1 M NaCl/0.1 M sodium acetate (pH 4.3) was added to the reaction sample. Additional incubation was at 37°C for 1 h. The sample was transferred to stop solution (1 M glycine, NaOH [pH 10.5]), and the plate was read at excitation 366 nm and emission 450 nm on a PerkinElmer Victor X4 plate reader (PerkinElmer, Waltham, MA). The activity was expressed as nanomoles of 4-methylumbelliferone released per hour per milliliter of plasma or milligram of protein. Protein concentration was determined by a bicinchoninic acid protein assay kit (Thermo Fisher Scientific, Waltham, MA).

Glycosaminoglycans assay

Glycosaminoglycans, mainly KS (biomarker of MPS IVA) levels in blood and tissues, were measured by liquid chromatography-tandem mass spectrometry (LC-MS/MS). Ten microliters of plasma/urine or standard and 90 μL of 50 mM Tris-HCl (pH 7.0) were added to wells of AcroPrep Advance 96-Well Filter Plates that have Ultrafiltration Omega 10 K membrane filters (PALL Corporation, NY). A cocktail of 40 μL with recombinant chondroitinase B, heparinase, and keratanase II (all enzymes, 1 mU/sample), and IS solution (5 μg/mL) was added to each well, followed by 60 μL of 50 mM Tris-HCl (pH 7.0) added to each well. The filter plate was placed on a 96-well plate and incubated at 37°C overnight. The plate was then centrifuged at 14.4 × *g* for 20 min. The samples were injected into LC-MS/MS. The apparatus consisted of a 1290 Infinity LC system coupled to a 6460 triple-quad mass spectrometer (Agilent Technologies, Palo Alto, CA). The injection volume was 5 μL, and a Hypercarb column (2.0 mm i.d., 50 mm, 5-μm; Thermo Fisher Scientific, Waltham, MA) was used at 60°C to separate disaccharides. The mobile phases were 100 mM ammonia (A) and 100% acetonitrile (B). The gradient condition was programmed as follows: the initial composition of 100% A was held for 1 min, linearly modified to 30% B to 4 min, maintained at 30% B to 5.5 min, returned to 0% B to 6 min, and maintained at 0% B until 10 min. The flow rate was 0.7 mL/min. Specific precursor and product ions, m/z, were used to quantify each disaccharide, respectively (IS, 354.3, 193.1; DS, 454.8, 300.2; mono-sulfated KS, 462, 97; di-sulfated KS, 542, 462; diHS-NS, 416, 138; diHS-0S, 378.3, 175.1).[59–61] The concentration of each disaccharide was calculated using QQQ Quantitative Analysis software. The levels of GAG in urine samples were normalized by creatinine, measured with a (urinary) Creatinine Colorimetric Assay Kit (Cayman Chemical, Ann Arbor, MI).[62–64]

Glycosaminoglycan extraction from tissue

Glycosaminoglycan extraction from tissue was performed as described earlier,[65] with minor modifications. Frozen mouse tissues (30–50 mg) were dissected and homogenized in cold acetone in homogenization tubes (2 mL microtubes pre-filled with 2.8-mm ceramic beads) by Omni Bead Ruptor Bead Mill Homogenizer (OMNI international, Kennesaw, GA) according to manufacturer-recommended speed and time. Tissue homogenate was transferred into a 1.5-mL tube and centrifuged for 30 min at 12,000 × *g*, at 4°C. The acetone buffer was removed, and de-fat pellets were dried (using a vacuum centrifuge). Two hundred microliters of 0.5 N NaOH were added to the dried pellet and were incubated for 2 h at 50°C to remove the attached GAG chains from its core protein. The mixture was neutralized with 1 N HCl (100 μL), NaCl powder was added to a final concentration of 3 M. The suspension was then centrifuged to remove nucleotides, and the pH of the supernatant was adjusted below 1.0

Figure 7. Bone pathology (knee joint)

Growth plate region (A), articular cartilage region (B), chondrocyte (300 for each group) cell size in growth plate lesions of femur (C), and tibia (D). Yellow asterisks indicate the representative non-vacuolated chondrocytes. Red asterisks indicate the representative chondrocytes vacuolated. Chondrocyte cell size in growth plate lesions of femur (C) and tibia (D) was quantified by ImageJ. Femur; UT vs. WT, AAV9co-CAG, and AAV8co-LMTP (****$p < 0.0001$), UT vs. AAV8co-V2-TBG, AAV9co-LMTP, and AAV9co-LBTP (*$p < 0.05$), UT vs. AAV8co-CAG (**$p < 0.01$). Tibia; UT vs. WT (****$p < 0.0001$), UT vs. AAV8co-CAG (*$p < 0.05$), AAV8co-V2-TBG vs. AAV8co-LSPX (*$p < 0.05$), and AAV8co-CAG vs. AAV9co-CAG (*$p < 0.05$). UT, untreated; WT, wild-type; TBG, thyroxin-binding globulin; LSPX, human alpha1-antitrypsin (hAAT); CAG, ubiquitous cytomegalovirus early enhancer/chicken β-actin; LMTP, liver-muscle tandem promoter; LBTP, liver-bone tandem promoter; GP, growth plate region; AC, articular cartilage region.

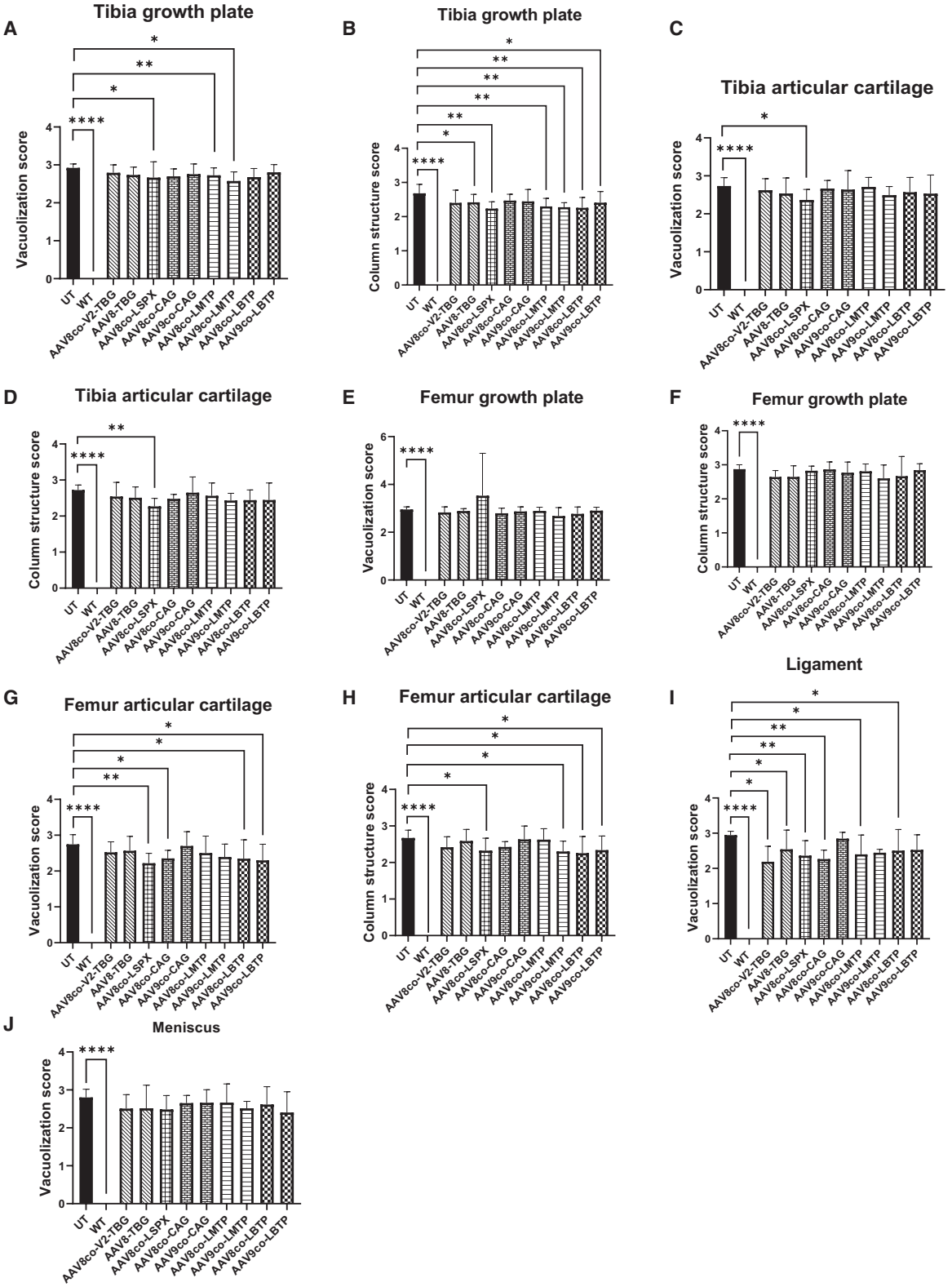

(legend on next page)

with 1 N HCl (83.3 μL) to precipitate proteins. After centrifugation, the supernatant was neutralized with 1 N NaOH (83.3 μL). The crude GAGs were precipitated by adding 2 volumes of ethanol containing 1.3% potassium acetate. After centrifugation, the precipitate was dried entirely and dissolved in 50 mM Tris-HCL (pH 7.0).

Detection of plasma anti-GALNS IgG antibodies

The presence of anti-hGALNS antibodies in plasma was assessed by the indirect ELISA method, as described previously.[19,66] Briefly, 96-well plates were coated with 2 μg/mL purified rhGALNS (R&D Systems, Minneapolis, MN) overnight in 15 mM Na_2CO_3, 35 mM $NaHCO_3$, and 0.02% NaN_3 (pH 9.6), and then blocked for 1 h at room temperature with 3% bovine serum albumin in PBS (pH 7.2). Diluted plasma (1:100) was added to the wells and incubated at 37°C for 2.5 h. The secondary antibody of peroxidase-conjugated goat anti-mouse immunoglobulin (Ig)G (Thermo Fisher Scientific, Waltham, MA) at a 1:1,000 dilution was added to the wells and incubated at room temperature for 1 h. Peroxidase substrate (ABTS solution, Invitrogen, Carlsbad, CA) was added, and plates were incubated for 30 min. The reaction was stopped by adding 1% sodium dodecyl sulfate (SDS), and the absorbance was read at an optical density of 410 nm on a PerkinElmer Victor X4 plate reader (PerkinElmer, Waltham, MA).

Quantification of AAV genome copies

The AAV genome copies in the tissues (liver, muscle, and bone) were quantified by the digital PCR method, as previously described.[19]

Assessment of bone pathology

Toluidine blue staining was performed as described previously.[67] Briefly, the knee joint was collected from MPS IVA and WT mice at 16 weeks old to evaluate levels of storage granules by light microscopy. Tissues were fixed in 2% paraformaldehyde and 4% glutaraldehyde in PBS, post-fixed in osmium tetroxide and embedded in Spurr's resin. Then, toluidine blue-stained 0.5-μm-thick sections were examined. Pathological slides from the knee joint of the treated and untreated MPS IVA and WT mice were evaluated to reduce vacuolization and improve column orientation in the growth plate. The amount of storage materials and the degree of disoriented columns were scored. Each pathological slide was assessed in a double-blind manner three times. We averaged the score in a group of mice per section of bone (growth plate, articular disc, meniscus, and ligament).

Micro-computed tomography analysis of femur

Micro-computed tomography (micro-CT) analysis of mice femurs was performed as described previously.[68] The femurs of male MPS IVA mice 12 weeks post-injection of AAV vectors were analyzed using the SkyScan 1275 system (Bruker, Billerica, MA) with a source voltage and current of 80 kV and 125 μA, respectively. Three-dimensional microstructural images were reconstructed using SkyScan NRecon software. Bruker CTAn software (Bruker Corporation, Billerica, MA) was used to calculate trabecular bone volume (BV/TV, %), trabecular number (Tb.N, 1/mm), and BMD (gHA/cm^3).

Data analysis

The statistical analysis was performed as t tests (and nonparametric tests) using GraphPad Prism 9.0 (GraphPad, San Diego, CA). All data are expressed as means and standard deviations. The statistical significance of the difference was considered as $p < 0.05$.

DATA AVAILABILITY

Any raw data generated in this study is available upon request.

ACKNOWLEDGMENTS

This work was supported by grants from the Austrian MPS Society, A Cure for Robert, Inc., The Carol Ann Foundation, Angelo R. Cali & Mary V. Cali Family Foundation, Inc., The Vain and Harry Fish Foundation, Inc., The Bennett Foundation, Jacob Randall Foundation, and Nemours. S.T. was supported by an Institutional Development Award from the Eunice Kennedy Shriver National Institute of Child Health & Human Development of the National Institutes of Health (NICHD) (1R01HD102545-01A1). This work was also supported by a sponsored research agreement from REGENXBIO.

AUTHOR CONTRIBUTIONS

S.A.K. and J.V.A. performed experiments in the mouse model. S.A.K. analyzed data, made figures, and wrote the first draft of the manuscript. F.N.U.N., E.B.F., and S.T. performed a pathological assessment in murine models. S.T. edited the manuscript. All authors read and approved the manuscript.

DECLARATION OF INTERESTS

All authors declare no competing interests.

SUPPLEMENTAL INFORMATION

Supplemental information can be found online at https://doi.org/10.1016/j.omtm.2025.101447.

REFERENCES

1. Matalon, R., Arbogast, B., Justice, P., Brandt, I.K., and Dorfman, A. (1974). Morquio's syndrome: deficiency of a chondroitin sulfate N-acetylhexosamine sulfate sulfatase. Biochem. Biophys. Res. Commun. *61*, 759–765.

Figure 8. Tibia and femur growth plate and articular cartilage score for vacuolization and column structure and ligament and meniscus vacuolization

One-way ANOVA. Tibia growth plate vacuolization score (A); UT vs. WT (****$p < 0.0001$), UT vs. AAV8co-LSPX and AAV9co-LMTP (*$p < 0.05$), UT vs. AAV8co-LMTP (**$p < 0.01$). Tibia growth plate column structure score (B); UT vs. WT (****$p < 0.0001$), UT vs. AAV8-TBG and AAV9co-LBTP (*$p < 0.05$), UT vs. AAV8co-LSPX, AAV8co-LMTP, AAV9co-LMTP and AAV8co-LBTP (**$p < 0.01$). Tibia articular cartilage vacuolization score (C); UT vs. WT (****$p < 0.0001$), UT vs. AAV8co-LSPX (*$p < 0.05$). Tibia articular cartilage column structure score (D); UT vs. WT (****$p < 0.0001$), UT vs. AAV8co-LSPX (**$p < 0.01$). Femur growth plate vacuolization score (E); UT vs. WT (****$p < 0.0001$). Femur growth plate column structure score (F); UT vs. WT (****$p < 0.0001$). Femur articular cartilage vacuolization score (G); UT vs. WT (****$p < 0.0001$), UT vs. AAV8co-LSPX (**$p < 0.01$), UT vs. AAV8co-CAG, AAV8co-LBTP, and AAV9co-LBTP (*$p < 0.05$). Femur articular cartilage column structure score (H); UT vs. WT (****$p < 0.0001$), UT vs. AAV8co-LSPX, AAV9co-LMTP, AAV8co-LBTP, and AAV9co-LBTP (*$p < 0.05$). Ligament vacuolization (I); UT vs. WT (****$p < 0.0001$), UT vs. AAV8co-V2-TBG, AAV8-TBG, AAV8co-LMTP, and AAV8co-LBTP (*$p < 0.05$), UT vs. AAV8co-LSPX and AAV8co-CAG (**$p < 0.01$). Meniscus vacuolization (J); UT vs. WT (****$p < 0.0001$). UT, untreated; WT, wild-type; TBG, thyroxin-binding globulin; LSPX, human alpha1-antitrypsin (hAAT); CAG, ubiquitous cytomegalovirus early enhancer/chicken β-actin; LMTP, liver-muscle tandem promoter; and LBTP, liver-bone tandem promoter.

2. Dorfman, A., Arbogast, B., and Matalon, R. (1976). The enzymic defects in Morquio and Maroteaux-Lamy syndrome. Adv. Exp. Med. Biol. *68*, 261–276.

3. Singh, J., Di Ferrante, N., Niebes, P., and Tavella, D. (1976). N-acetylgalactosamine-6-sulfate sulfatase in man. Absence of the enzyme in Morquio disease. J. Clin. Investig. *57*, 1036–1040.

4. Di Ferrante, N., Ginsberg, L.C., Donnelly, P.V., Di Ferrante, D.T., and Caskey, C.T. (1978). Deficiencies of glucosamine-6-sulfate or galactosamine-6-sulfate sulfatases are responsible for different mucopolysaccharidoses. Science *199*, 79–81.

5. Montano, A.M., Tomatsu, S., Gottesman, G.S., Smith, M., and Orii, T. (2007). International Morquio A Registry: clinical manifestation and natural course of Morquio A disease. J. Inherit. Metab. Dis. *30*, 165–174.

6. Solanki, G.A., Martin, K.W., Theroux, M.C., Lampe, C., White, K.K., Shediac, R., Lampe, C.G., Beck, M., Mackenzie, W.G., Hendriksz, C.J., and Harmatz, P.R. (2013). Spinal involvement in mucopolysaccharidosis IVA (Morquio-Brailsford or Morquio A syndrome): presentation, diagnosis and management. J. Inherit. Metab. Dis. *36*, 339–355.

7. Charrow, J., Alden, T.D., Breathnach, C.A.R., Frawley, G.P., Hendriksz, C.J., Link, B., Mackenzie, W.G., Manara, R., Offiah, A.C., Solano, M.L., and Theroux, M. (2015). Diagnostic evaluation, monitoring, and perioperative management of spinal cord compression in patients with Morquio syndrome. Mol. Genet. Metab. *114*, 11–18.

8. Melbouci, M., Mason, R.W., Suzuki, Y., Fukao, T., Orii, T., and Tomatsu, S. (2018). Growth impairment in mucopolysaccharidoses. Mol. Genet. Metab. *124*, 1–10.

9. Lavery, C., and Hendriksz, C. (2015). Mortality in patients with morquio syndrome a. JIMD Rep. *15*, 59–66.

10. Pizarro, C., Davies, R.R., Theroux, M., Spurrier, E.A., Averill, L.W., and Tomatsu, S. (2016). Surgical Reconstruction for Severe Tracheal Obstruction in Morquio A Syndrome. Ann. Thorac. Surg. *102*, e329–e331.

11. Tomatsu, S., Averill, L.W., Sawamoto, K., Mackenzie, W.G., Bober, M.B., Pizarro, C., Goff, C.J., Xie, L., Orii, T., and Theroux, M. (2016). Obstructive airway in Morquio A syndrome, the past, the present and the future. Mol. Genet. Metab. *117*, 150–156.

12. Yasuda, E., Fushimi, K., Suzuki, Y., Shimizu, K., Takami, T., Zustin, J., Patel, P., Ruhnke, K., Shimada, T., Boyce, B., et al. (2013). Pathogenesis of Morquio A syndrome: an autopsied case reveals systemic storage disorder. Mol. Genet. Metab. *109*, 301–311.

13. Averill, L.W., Kecskemethy, H.H., Theroux, M.C., Mackenzie, W.G., Pizarro, C., Bober, M.B., Ditro, C.P., and Tomatsu, S. (2021). Tracheal narrowing in children and adults with mucopolysaccharidosis type IVA: evaluation with computed tomography angiography. Pediatr. Radiol. *51*, 1202–1213.

14. Doherty, C., Stapleton, M., Piechnik, M., Mason, R.W., Mackenzie, W.G., Yamaguchi, S., Kobayashi, H., Suzuki, Y., and Tomatsu, S. (2019). Effect of enzyme replacement therapy on the growth of patients with Morquio A. J. Hum. Genet. *64*, 625–635.

15. Chinen, Y., Higa, T., Tomatsu, S., Suzuki, Y., Orii, T., and Hyakuna, N. (2014). Long-term therapeutic efficacy of allogenic bone marrow transplantation in a patient with mucopolysaccharidosis IVA. Mol. Genet. Metab. Rep. *1*, 31–41.

16. Yabe, H., Tanaka, A., Chinen, Y., Kato, S., Sawamoto, K., Yasuda, E., Shintaku, H., Suzuki, Y., Orii, T., and Tomatsu, S. (2016). Hematopoietic stem cell transplantation for Morquio A syndrome. Mol. Genet. Metab. *117*, 84–94.

17. Wang, J., Luan, Z., Jiang, H., Fang, J., Qin, M., Lee, V., and Chen, J. (2016). Allogeneic Hematopoietic Stem Cell Transplantation in Thirty-Four Pediatric Cases of Mucopolysaccharidosis-A Ten-Year Report from the China Children Transplant Group. Biol. Blood Marrow Transplant. *22*, 2104–2108.

18. Wang, Z., Xu, Y., Jiang, E., Wang, J., Tomatsu, S., and Shen, K. (2020). Pathophysiology of Hip Disorders in Patients with Mucopolysaccharidosis IVA. Diagnostics *10*, 264.

19. Sawamoto, K., Karumuthil-Melethil, S., Khan, S., Stapleton, M., Bruder, J.T., Danos, O., and Tomatsu, S. (2020). Liver-Targeted AAV8 Gene Therapy Ameliorates Skeletal and Cardiovascular Pathology in a Mucopolysaccharidosis IVA Murine Model. Mol. Ther. Methods Clin. Dev. *18*, 50–61.

20. Colella, P., Sellier, P., Costa Verdera, H., Puzzo, F., van Wittenberghe, L., Guerchet, N., Daniele, N., Gjata, B., Marmier, S., Charles, S., et al. (2019). AAV Gene Transfer with Tandem Promoter Design Prevents Anti-transgene Immunity and Provides Persistent Efficacy in Neonate Pompe Mice. Mol. Ther. Methods Clin. Dev. *12*, 85–101.

21. Piechnik, M., Amendum, P.C., Sawamoto, K., Stapleton, M., Khan, S., Fnu, N., Álvarez, V., Pachon, A.M.H., Danos, O., Bruder, J.T., et al. (2022). Sex Difference Leads to Differential Gene Expression Patterns and Therapeutic Efficacy in Mucopolysaccharidosis IVA Murine Model Receiving AAV8 Gene Therapy. Int. J. Mol. Sci. *23*, 12693.

22. Domenger, C., and Grimm, D. (2019). Next-generation AAV vectors-do not judge a virus (only) by its cover. Hum. Mol. Genet. *28*, R3–R14.

23. Ozelo, M.C., Mahlangu, J., Pasi, K.J., Giermasz, A., Leavitt, A.D., Laffan, M., Symington, E., Quon, D.V., Wang, J.D., Peerlinck, K., et al. (2022). Valoctocogene Roxaparvovec Gene Therapy for Hemophilia A. N. Engl. J. Med. *386*, 1013–1025.

24. Vandendriessche, T., Thorrez, L., Acosta-Sanchez, A., Petrus, I., Wang, L., Ma, L., De Waele, L., Iwasaki, Y., Gillijns, V., Wilson, J.M., et al. (2007). Efficacy and safety of adeno-associated viral vectors based on serotype 8 and 9 vs. lentiviral vectors for hemophilia B gene therapy. J. Thromb. Haemost. *5*, 16–24.

25. Arabi, F., Mansouri, V., and Ahmadbeigi, N. (2022). Gene therapy clinical trials, where do we go? An overview. Biomed. Pharmacother. *153*, 113324.

26. Tessitore, A., Faella, A., O'Malley, T., Cotugno, G., Doria, M., Kunieda, T., Matarese, G., Haskins, M., and Auricchio, A. (2008). Biochemical, pathological, and skeletal improvement of mucopolysaccharidosis VI after gene transfer to liver but not to muscle. Mol. Ther. *16*, 30–37.

27. Ferla, R., O'Malley, T., Calcedo, R., O'Donnell, P., Wang, P., Cotugno, G., Claudiani, P., Wilson, J.M., Haskins, M., and Auricchio, A. (2013). Gene therapy for mucopolysaccharidosis type VI is effective in cats without pre-existing immunity to AAV8. Hum. Gene Ther. *24*, 163–169.

28. Wang, D., Tai, P.W.L., and Gao, G. (2019). Adeno-associated virus vector as a platform for gene therapy delivery. Nat. Rev. Drug Discov. *18*, 358–378.

29. Wood, S.R., and Bigger, B.W. (2022). Delivering gene therapy for mucopolysaccharide diseases. Front. Mol. Biosci. *9*, 965089.

30. Colella, P., Ronzitti, G., and Mingozzi, F. (2018). Emerging Issues in AAV-Mediated In Vivo Gene Therapy. Mol. Ther. Methods Clin. Dev. *8*, 87–104.

31. Nieuwenhuis, B., Haenzi, B., Hilton, S., Carnicer-Lombarte, A., Hobo, B., Verhaagen, J., and Fawcett, J.W. (2021). Optimization of adeno-associated viral vector-mediated transduction of the corticospinal tract: comparison of four promoters. Gene Ther. *28*, 56–74.

32. Nieuwenhuis, B., Laperrousaz, E., Tribble, J.R., Verhaagen, J., Fawcett, J.W., Martin, K.R., Williams, P.A., and Osborne, A. (2023). Improving adeno-associated viral (AAV) vector-mediated transgene expression in retinal ganglion cells: comparison of five promoters. Gene Ther. *30*, 503–519.

33. Yang, Y.S., Xie, J., Wang, D., Kim, J.M., Tai, P.W.L., Gravallese, E., Gao, G., and Shim, J.H. (2019). Bone-targeting AAV-mediated silencing of Schnurri-3 prevents bone loss in osteoporosis. Nat. Commun. *10*, 2958.

34. Chen, Q., Luo, H., Zhou, C., Yu, H., Yao, S., Fu, F., Seeley, R., Ji, X., Yang, Y., Chen, P., et al. (2020). Comparative intra-articular gene transfer of seven adeno-associated virus serotypes reveals that AAV2 mediates the most efficient transduction to mouse arthritic chondrocytes. PLoS One *15*, e0243359.

35. Zincarelli, C., Soltys, S., Rengo, G., and Rabinowitz, J.E. (2008). Analysis of AAV serotypes 1-9 mediated gene expression and tropism in mice after systemic injection. Mol. Ther. *16*, 1073–1080.

36. Bertolin, J., Sánchez, V., Ribera, A., Jaén, M.L., Garcia, M., Pujol, A., Sánchez, X., Muñoz, S., Marcó, S., Pérez, J., et al. (2021). Treatment of skeletal and non-skeletal alterations of Mucopolysaccharidosis type IVA by AAV-mediated gene therapy. Nat. Commun. *12*, 5343.

37. Tomatsu, S., Orii, K.O., Vogler, C., Nakayama, J., Levy, B., Grubb, J.H., Gutierrez, M.A., Shim, S., Yamaguchi, S., Nishioka, T., et al. (2003). Mouse model of N-acetylgalactosamine-6-sulfate sulfatase deficiency (Galns-/-) produced by targeted disruption of the gene defective in Morquio A disease. Hum. Mol. Genet. *12*, 3349–3358.

38. Paneda, A., Vanrell, L., Mauleon, I., Crettaz, J.S., Berraondo, P., Timmermans, E.J., Beattie, S.G., Twisk, J., van Deventer, S., Prieto, J., et al. (2009). Effect of

adeno-associated virus serotype and genomic structure on liver transduction and biodistribution in mice of both genders. Hum. Gene Ther. *20*, 908–917.

39. Nam, H.J., Lane, M.D., Padron, E., Gurda, B., McKenna, R., Kohlbrenner, E., Aslanidi, G., Byrne, B., Muzyczka, N., Zolotukhin, S., and Agbandje-McKenna, M. (2007). Structure of adeno-associated virus serotype 8, a gene therapy vector. J. Virol. *81*, 12260–12271.
40. Cabanes-Creus, M., Navarro, R.G., Zhu, E., Baltazar, G., Liao, S.H.Y., Drouyer, M., Amaya, A.K., Scott, S., Nguyen, L.H., Westhaus, A., et al. (2022). Novel human liver-tropic AAV variants define transferable domains that markedly enhance the human tropism of AAV7 and AAV8. Mol. Ther. Methods Clin. Dev. *24*, 88–101.
41. Nakai, H., Fuess, S., Storm, T.A., Muramatsu, S.i., Nara, Y., and Kay, M.A. (2005). Unrestricted hepatocyte transduction with adeno-associated virus serotype 8 vectors in mice. J. Virol. *79*, 214–224.
42. Thomas, C.E., Storm, T.A., Huang, Z., and Kay, M.A. (2004). Rapid uncoating of vector genomes is the key to efficient liver transduction with pseudotyped adeno-associated virus vectors. J. Virol. *78*, 3110–3122.
43. Nam, H.J., Gurda, B.L., McKenna, R., Potter, M., Byrne, B., Salganik, M., Muzyczka, N., and Agbandje McKenna, M. (2011). Structural studies of adeno-associated virus serotype 8 capsid transitions associated with endosomal trafficking. J. Virol. *85*, 11791–11799.
44. Monahan, P.E., Lothrop, C.D., Sun, J., Hirsch, M.L., Kafri, T., Kantor, B., Sarkar, R., Tillson, D.M., Elia, J.R., and Samulski, R.J. (2010). Proteasome inhibitors enhance gene delivery by AAV virus vectors expressing large genomes in hemophilia mouse and dog models: a strategy for broad clinical application. Mol. Ther. *18*, 1907–1916.
45. Jiang, H., Couto, L.B., Patarroyo-White, S., Liu, T., Nagy, D., Vargas, J.A., Zhou, S., Scallan, C.D., Sommer, J., Vijay, S., et al. (2006). Effects of transient immunosuppression on adenoassociated, virus-mediated, liver-directed gene transfer in rhesus macaques and implications for human gene therapy. Blood *108*, 3321–3328.
46. Wang, Z., Zhu, T., Qiao, C., Zhou, L., Wang, B., Zhang, J., Chen, C., Li, J., and Xiao, X. (2005). Adeno-associated virus serotype 8 efficiently delivers genes to muscle and heart. Nat. Biotechnol. *23*, 321–328.
47. Wu, Z., Asokan, A., and Samulski, R.J. (2006). Adeno-associated virus serotypes: vector toolkit for human gene therapy. Mol. Ther. *14*, 316–327.
48. Gao, G., Vandenberghe, L.H., Alvira, M.R., Lu, Y., Calcedo, R., Zhou, X., and Wilson, J.M. (2004). Clades of Adeno-associated viruses are widely disseminated in human tissues. J. Virol. *78*, 6381–6388.
49. Michelfelder, S., and Trepel, M. (2009). Adeno-associated viral vectors and their redirection to cell-type specific receptors. Adv. Genet. *67*, 29–60.
50. Foust, K.D., Nurre, E., Montgomery, C.L., Hernandez, A., Chan, C.M., and Kaspar, B.K. (2009). Intravascular AAV9 preferentially targets neonatal neurons and adult astrocytes. Nat. Biotechnol. *27*, 59–65.
51. Gray, S.J., Matagne, V., Bachaboina, L., Yadav, S., Ojeda, S.R., and Samulski, R.J. (2011). Preclinical differences of intravascular AAV9 delivery to neurons and glia: a comparative study of adult mice and nonhuman primates. Mol. Ther. *19*, 1058–1069.
52. Bevan, A.K., Duque, S., Foust, K.D., Morales, P.R., Braun, L., Schmelzer, L., Chan, C.M., McCrate, M., Chicoine, L.G., Coley, B.D., et al. (2011). Systemic gene delivery in large species for targeting spinal cord, brain, and peripheral tissues for pediatric disorders. Mol. Ther. *19*, 1971–1980.
53. Duque, S., Joussemet, B., Riviere, C., Marais, T., Dubreil, L., Douar, A.M., Fyfe, J., Moullier, P., Colle, M.A., and Barkats, M. (2009). Intravenous administration of self-complementary AAV9 enables transgene delivery to adult motor neurons. Mol. Ther. *17*, 1187–1196.
54. Pacak, C.A., Mah, C.S., Thattaliyath, B.D., Conlon, T.J., Lewis, M.A., Cloutier, D.E., Zolotukhin, I., Tarantal, A.F., and Byrne, B.J. (2006). Recombinant adeno-associated virus serotype 9 leads to preferential cardiac transduction in vivo. Circ. Res. *99*, e3–e9.
55. Asokan, A., Schaffer, D.V., and Samulski, R.J. (2012). The AAV vector toolkit: poised at the clinical crossroads. Mol. Ther. *20*, 699–708.
56. Pleger, S.T., Shan, C., Ksienzyk, J., Bekeredjian, R., Boekstegers, P., Hinkel, R., Schinkel, S., Leuchs, B., Ludwig, J., Qiu, G., et al. (2011). Cardiac AAV9-S100A1 gene therapy rescues post-ischemic heart failure in a preclinical large animal model. Sci. Transl. Med. *3*, 92ra64.
57. Bish, L.T., Morine, K., Sleeper, M.M., Sanmiguel, J., Wu, D., Gao, G., Wilson, J.M., and Sweeney, H.L. (2008). Adeno-associated virus (AAV) serotype 9 provides global cardiac gene transfer superior to AAV1, AAV6, AAV7, and AAV8 in the mouse and rat. Hum. Gene Ther. *19*, 1359–1368.
58. Inagaki, K., Fuess, S., Storm, T.A., Gibson, G.A., McTiernan, C.F., Kay, M.A., and Nakai, H. (2006). Robust systemic transduction with AAV9 vectors in mice: efficient global cardiac gene transfer superior to that of AAV8. Mol. Ther. *14*, 45–53.
59. Oguma, T., Tomatsu, S., Montano, A.M., and Okazaki, O. (2007). Analytical method for the determination of disaccharides derived from keratan, heparan, and dermatan sulfates in human serum and plasma by high-performance liquid chromatography/turbo ionspray ionization tandem mass spectrometry. Anal. Biochem. *368*, 79–86.
60. Oguma, T., Toyoda, H., Toida, T., and Imanari, T. (2001). Analytical method for keratan sulfates by high-performance liquid chromatography/turbo-ionspray tandem mass spectrometry. Anal. Biochem. *290*, 68–73.
61. Oguma, T., Tomatsu, S., and Okazaki, O. (2007). Analytical method for determination of disaccharides derived from keratan sulfates in human serum and plasma by high-performance liquid chromatography/turbo-ionspray ionization tandem mass spectrometry. Biomed. Chromatogr. *21*, 356–362.
62. Tomatsu, S., Shimada, T., Mason, R.W., Montaño, A.M., Kelly, J., LaMarr, W.A., Kubaski, F., Giugliani, R., Guha, A., Yasuda, E., et al. (2014). Establishment of glycosaminoglycan assays for mucopolysaccharidoses. Metabolites *4*, 655–679.
63. Hintze, J.P., Tomatsu, S., Fujii, T., Montaño, A.M., Yamaguchi, S., Suzuki, Y., Fukushi, M., Ishimaru, T., and Orii, T. (2011). Comparison of liquid chromatography-tandem mass spectrometry and sandwich ELISA for determination of keratan sulfate in plasma and urine. Biomark. Insights *6*, 69–78.
64. Khan, S.A., Mason, R.W., Giugliani, R., Orii, K., Fukao, T., Suzuki, Y., Yamaguchi, S., Kobayashi, H., Orii, T., and Tomatsu, S. (2018). Glycosaminoglycans analysis in blood and urine of patients with mucopolysaccharidosis. Mol. Genet. Metab. *125*, 44–52.
65. Mochizuki, H., Yoshida, K., Shibata, Y., and Kimata, K. (2008). Tetrasulfated disaccharide unit in heparan sulfate: enzymatic formation and tissue distribution. J. Biol. Chem. *283*, 31237–31245.
66. Tomatsu, S., Orii, K.O., Vogler, C., Grubb, J.H., Snella, E.M., Gutierrez, M., Dieter, T., Holden, C.C., Sukegawa, K., Orii, T., et al. (2003). Production of MPS VII mouse (Gus(tm(hE540A x mE536A)Sly)) doubly tolerant to human and mouse beta-glucuronidase. Hum. Mol. Genet. *12*, 961–973.
67. Tomatsu, S., Gutierrez, M., Nishioka, T., Yamada, M., Yamada, M., Tosaka, Y., Grubb, J.H., Montaño, A.M., Vieira, M.B., Trandafirescu, G.G., et al. (2005). Development of MPS IVA mouse (Galnstm(hC79S.mC76S)slu) tolerant to human N-acetylgalactosamine-6-sulfate sulfatase. Hum. Mol. Genet. *14*, 3321–3335.
68. Santi, L., De Ponti, G., Dina, G., Pievani, A., Corsi, A., Riminucci, M., Khan, S., Sawamoto, K., Antolini, L., Gregori, S., et al. (2020). Neonatal combination therapy improves some of the clinical manifestations in the Mucopolysaccharidosis type I murine model. Mol. Genet. Metab. *130*, 197–208.